



PhD THESIS

ECO-FRIENDLY GEOPOLYMER MATERIALS BASED ON INDUSTRIAL WASTE AND BY- PRODUCTS

Author:

PhD Student Eng. Nicolaie MARIN

Research Supervisor:

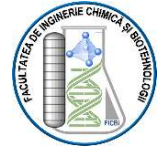
Prof. Habil.Dr. Eng. Cristina ORBECI

DOCTORAL COMMITTEE

President	Prof. Dr. Eng. Ileana RĂU	from	National University of Science and Technology Politehnica Bucharest
Research Supervisor	Prof. Dr. Eng. Cristina ORBECI	from	National University of Science and Technology Politehnica Bucharest
Member	Conf. Dr. Eng. Larisa Mădălina MELIȚĂ	from	Technical University of Civil Engineering Bucharest
Member	CS II Dr. Lidia KIM	from	National Research and Development Institute for Industrial Ecology – INCD ECOIND
Member	Conf. Dr. Eng. Constantin BOBIRICĂ	from	National University of Science and Technology Politehnica Bucharest



National University of Science and Technology
POLITEHNICA Bucharest
FACULTY OF CHEMICAL ENGINEERING AND
BIOTECHNOLOGIES
Doctoral School Chemical Engineering and
Biotechnologies



PhD THESIS Summary

ECO-FRIENDLY GEOPOLYMER MATERIALS BASED
ON INDUSTRIAL WASTE AND BY- PRODUCTS

Author:

PhD Student Eng. Nicolaie MARIN

Research Supervisor:

Prof. Habil.Dr. Eng. Cristina ORBECI

CONTENTS

Introduction.....	8
Chapter I. Current state of knowledge regarding the manufacture of geopolymers from industrial waste and by-products.....	11
I.1. General.....	11
I.2. Description of the geopolymerization process	14
I.3. The mechanism of the geopolymerization process	15
I.4. Raw materials used as geopolymer precursors	18
I.5. Types of alkaline activators used in the manufacture of geopolymers	20
I.5.1. Conventional activators	20
I.5.2. Alternative Activators	23
Chapter II. Features of power plant ash and red mud	Error! Bookmark not defined.26
II.1. Features of thermal power plant ash.....	27
II.1.1. General aspects.....	27
II.1.2. Bottom ash.....	28
II.1.3. Light or flying ash (fly ash)	32
II.2. Features of red mud	40
Chapter III. Characteristics of glass waste type WEEE.....	Error! Bookmark not defined.45
III.1. Glass waste from cathode ray tubes (CRT)	45
III.1.1. General aspects.....	45
III.1.2. Physicochemical characteristics of CRT glass.....	50
III.2. Glass waste from fluorescent lamps	53
III.2.1. General aspects.....	53
III.2.2. Features of fluorescent lamps	53
III.2.3. Tratarea deșeurilor de tipul lămpilor fluorescente scoase din uz	60
Research objectives.....	64
Chapter IV. Preparation of “two-part” geopolymers based on light ash and addition of glass as additional active material.....	66
IV.1. Specific objectives	66
IV.2. Materials and methods	66
IV.2.1. Materials.....	66
IV.2.2. Preparation of geopolymer assortments.....	69
IV.2.3. Analysis and test methods.....	70
IV.3. Results and discussion.....	72
IV.3.1. Leaching behaviour test.....	72
IV.3.2. Compressive strength testing.....	73
IV.3.3. Morphological and structural characterization	74

IV.4. Partial conclusions	85
Chapter V. Preparation of “one-part” geopolymers based on light ash and addition of red mud using alternative solid activators based on glass waste	86
V.1. Specific objectives	86
V.2. Materials and methods	87
V.2.1. Materials	87
V.2.2. Synthesis of solid alkaline activators	87
V.2.3. Preparation of one-part cements based on red mud and light ash	88
V.2.4. Characterisation and testing of prepared solid alkaline activators and “one-part” geopolymers	90
V.3. Results and discussion	92
V.3.1. Water solubility	92
V.3.2. Characterisation of solid activators	95
V.3.3. Test of solid activators for the manufacture of “one-part” geopolymers based on light ash and addition of red mud	105
V.4. Partial conclusions	111
Chapter VI. Evaluation of long-term leaching behaviour of “one-part” geopolymers based on conformity leaching tests	112
VI.1. Specific objectives	112
VI.2. Materials and methods	113
VI.2.1. Material	113
VI.2.2. Synthesis of solid activators	114
VI.2.3. Preparation of one-part geopolymers to be tested	114
VI.2.4. Teste de levigare	115
VI. 3. Results and discussion	116
VI.3.1. Description of the leaching model	116
V.3.2. TCLP test results	118
VI.3.3. Assessment of long-term leaching behaviour	119
VI.4. Partial conclusion	124
VII. General conclusions	125
Original contributions and prospects for further development	127
Dissemination of experimental research results	129
Bibliography	131
List of figures	149
List of tables	152

Introduction

In the context of the circular economy and more intense efforts at the European and global level to reduce the carbon footprint, secondary raw materials are becoming increasingly important. They are sought to reduce the exploitation of natural resources and to enhance sustainability. The construction sector, in particular, is adopting the use of secondary raw materials, partially or totally replacing natural raw materials with various by-products and industrial waste. An example is the industry of inorganic binders based on cement, which uses industrial waste such as power plant ash and furnace slag to reduce the carbon footprint associated with the manufacturing process. This doctoral thesis focuses on the valorization of secondary raw materials and explores the obtaining of new materials, especially geopolymers, using almost exclusively waste and industrial by-products. Chapter I of the thesis presents the current state of knowledge regarding the manufacture of geopolymers from secondary raw materials, describing the geopolymerization process and the mechanism of alkaline activation of geopolymetric precursors. Also detailed are the secondary raw materials frequently used in the manufacture of geopolymers and the categories of alkaline activators used in their activation process. In Chapter II, two types of glass waste used in the synthesis of new types of geopolymers studied in this doctoral thesis are presented. The physico-chemical characteristics of the glass waste from the cathode tubes of televisions and monitors taken out of use (CRT type glass) and the waste glass from the fluorescent lamps taken out of use are detailed. Also discussed are the main methods of treating these wastes, either for their valorization or for the removal of hazardous components. Chapter III presents experimental data related to the synthesis and characterization of “two-part” type geopolymer assortments based on light power plant ash, with an active addition of glass waste from fluorescent lamps taken out of use. The method of designing the synthesis mixtures, the actual synthesis process is described, and the geopolymers are characterized. Chapter IV of the doctoral thesis presents the experimental results obtained with reference to the synthesis and characterization of “one-part” type geopolymer assortments based on light power plant ash and red mud. Also described is the procedure for obtaining a solid alkaline activator based on CRT type glass waste by alkaline fusion with sodium hydroxide. The synthesis products obtained are characterized structurally and morphologically, highlighting their performances. In Chapter V, a detailed experimental study on the leaching behavior of one-part type geopolymers is presented. These geopolymers are obtained from light power plant ash and red mud, activated with a solid alkaline activator based on CRT type glass waste. The chapter describes the leaching testing procedure and the models used to estimate the long-term mobility of contaminants contained in secondary raw materials. Also presented are details regarding the leaching behavior of contaminants in the obtained geopolymers, highlighting their performances under aggressive environmental conditions. Chapter VI contains the general conclusions of the experimental research within the doctoral thesis, as well as the original contributions and perspectives for further development in accordance with the studied theme.

At the end of the thesis there is highlighted the original contribution of the research, the directions of continuation of the study, the list of published papers and conferences where the experimental results were communicated, as well as the bibliographic sources consulted.

The thesis has 152 pages, 39 figures, 18 tables and 163 bibliographic sources.

The doctoral thesis was capitalized through 3 publications, of which 2 articles in ISI indexed journals and 1 article in the Scientific Bulletin of POLITEHNICA Bucharest. At the same time, the results were communicated at 2 international conferences.

Keywords: glass waste, alkaline fusion, solid activators, fly ash, bottom ash, red mud, alkalinely activated monocomponent materials, fluorescent lamps, geopolymer, heavy metals, leaching behavior.

Part I. DOCUMENTARY STUDY

Chapter I. Current state of knowledge regarding the manufacture of geopolymers from industrial waste and by-products

I.1. General aspect

The large amount of waste generated today is a serious problem for the environment and the population. The acquisition of construction materials (especially Portland cement) involves the extraction of non-renewable raw materials such as limestone and clay, with high energy consumption. The total consumption of these is about 20 billion tons per year, and concrete production represents more than a third of this consumption. Because the cost of raw materials depends on the transport distance, there is a tendency to exploit them as close as possible to the sites, which increases the number of quarries and the impact on biodiversity. The use of secondary raw materials is becoming increasingly important to reduce the consumption of natural resources and enhance economic sustainability.

Geopolymerization is a simple technique for obtaining construction materials similar to Portland cement, using industrial waste as a source of raw materials. Through chemical reactions, polymeric structures of the type Si-O-Al and Si-O-Si are formed, balanced by alkaline ions. Geopolymers are inorganic polymers, obtained by alkaline activation of aluminosilicate materials, with a variable microstructure depending on the manufacturing parameters.

Geopolymers, ecological materials used in construction, have excellent mechanical properties and a reduced carbon footprint. They have found applications in various industries, including replacing traditional materials. An interesting aspect is their self-repair capacity. They have excellent properties, such as resistance to corrosion and fire, low thermal conductivity, and the ability to immobilize hazardous contaminants. Through the mechanism of geopolymerization, defects (cracks) are repaired, and mechanical properties gradually increase over time. Demolition and construction residues can be a potential source of precursors for geopolymers. As shown above, the main advantage (Figure 1) of using geopolymer binders is the reduced fuel consumption and the reduction of carbon dioxide emissions by 80% to 90%.

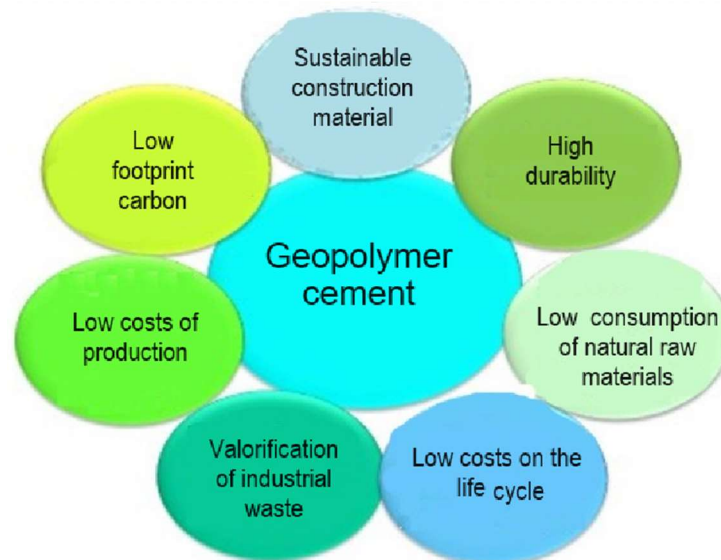


Figure 1. Advantages of geopolymer cement (Singh, 2022).

Geopolymer cement, obtained from industrial waste and by-products, has multiple advantages: low fuel consumption and CO₂ emissions, excellent durability, increased profitability, superior strength and ability to withstand fire. Geopolymer cement

constructions require less maintenance and are suitable for various projects, from roads to bridges and buildings.

I.2. Description of the geopolymerisation process

Geopolymers are inorganic, ceramic materials made up of covalent, non-crystalline (amorphous) lattices. They can be obtained from industrial waste and by-products. Geopolymers exhibit excellent properties, such as corrosion and fire resistance, and can be used in various construction projects, from roads to bridges and buildings. An example of a geopolymer is sialate (silicon-oxo-aluminate), with a structure consisting of tetrahedrons of SiO_4 and AlO_4 . The positive ions, Na^+ , K^+ and Ca_2^+ , balance the negative charge of Al_3^+ in the structure.

I.3. The mechanism of the geopolymerization process

Geopolymerization involves converting raw material (aluminosilicates) by dissolution into an alkaline solution. This solution forms a complex mixture of silicate, aluminatic and aluminosilicate species, and then the gel phase is formed. Water plays the role of reaction medium, and gelling time varies depending on conditions and composition.

Part II. ORIGINAL CONTRIBUTIONS

Research objectives

The main objectives of the doctoral thesis were:

Obtaining ecological geopolymers using secondary raw materials (light power plant ash, red mud, and glass waste) through activation with classic and alternative activators. This objective was achieved by preparing “two-part” and “one-part” type geopolymers, synthesizing alternative solid activators based on glass waste, and characterizing them.

Examining the technical performances of the obtained geopolymers to identify opportunities for valorization in the construction field. This objective was achieved by preliminary conditioning and characterization of raw materials, as well as by physico-chemical characterization of “two-part” and “one-part” type geopolymers.

Evaluating the long-term leaching behavior of the obtained geopolymers to determine their hazardous potential in relation to the environment. This objective was achieved by testing the leaching behavior of geopolymers and evaluating their long-term behavior based on leaching tests and models.

These results underline the potential for valorizing waste in the production of ecological geopolymers, offering a sustainable alternative in the construction sector.

Chapter IV. Preparation of two-part geopolymers based on light ash and addition of glass as additional active material

IV.1. Specific objectives

The main objectives of this chapter were:

- ✓ Physicochemical characterization of raw materials used for the preparation of assortments of geopolymers with liquid activators.
- ✓ Preparation of geopolymers based on light ash from thermal power plant and addition of waste glass using liquid activators.
- ✓ Testing the mechanical performance and leaching behavior of the obtained geopolymers.
- ✓ Characterization of geopolymers obtained by morphological and mineralogical analysis.
- ✓ Analysis of the obtained results and evaluation of the applicative potential of the obtained geopolymer assortments.

IV.2. Materials and methods

IV.2.1. Material

For the preparation of geopolymers, light F-class ash from a coal-fired power plant and glass waste from end-of-life linear fluorescent lamps were used. The glass, coated inside with a thin layer of fluorescent powder, was added to the powdered system to replace the fly ash. The glass was crushed and ground to a particle size of less than 74 μm .

The oxide composition and other chemical and physical properties of the raw materials are presented in Table 10. The technical characteristics of end-of-life fluorescent lamps are presented in Table 11.

For the safe processing of fluorescent lamps, a shredding system has been designed that allows the recovery of mercury found in the vapor phase inside them. Each fluorescent tube was inserted into a reinforced polyvinyl chloride tube, connected to a bottle with an acid mixture solution. Before grinding, a peristaltic pump was set at maximum speed for 10 minutes to pass mercury vapor into the acid solution. At the end

of each operation, the caps at the ends of the fluorescent tube were separated and the crushed glass was collected and prepared for grinding.

IV.2.2. Preparation of geopolymers

Five different types of geopolymers were created, depending on the percentage of light ash replaced by glass powder: 0%, 5%, 10%, 15% and 25% (mass). All grades were prepared at the same L-S mass ratio of 0.35. Light ash and glass powder were mixed manually in dry phase, then mixed with the activator. The resulting paste was poured into cylindrical formwork and vibrated for 2 minutes. The formwork was sealed and dried at 60°C for 24 hours, then stored at 20°C for another 24 hours. After removal from the formwork, the samples were sealed again and maintained at 20°C for a further 26 days. For each assortment, duplicate samples were prepared. Further details on these mixtures are presented in Table 12.

IV.2.3. Methods of analysis and testing

After a drying time of 28 days, according to standards, the geopolymer samples were subjected to a series of physical and chemical tests. These included compressive strength testing according to the standard procedure for cylindrical samples (ASTM C39/C39M-14) and evaluation of leaching behavior in relation to contained mercury according to the TCLP leaching compliance test (Method 1311).

The total mercury content of the raw materials and the analysis of mercury in leachates were determined according to the standard procedure for the determination of mercury in solid or semi-solid waste (Method 7471B) using a contraAA-300 atomic absorption spectrometer (Analytik-Jena, Germany).

The chemical composition of the raw materials was determined by X-ray fluorescence (XRF) on a Pioneer S4 spectrophotometer (Bruker AXS, Germany). Nitrogen adsorption-desorption isotherms were determined at 77.35 K on the Autosorb-iQ 2ST/MP analyzer (Quantachrome Instruments, USA), and surfaces were calculated from isotherms using the Brunauer-Emmett-Teller (BET) method.

Mineralogical analysis of anhydrous powder materials was performed by X-ray diffractometry (XRD) using a Bruker AXS D5005 goniometer (Bruker, Germany). Morphological observations of geopolymers were performed using a field-emission scanning electron microscope SUPRA 55VP (Carl Zeiss, Germany). The samples were coated with platinum powder with a spray coating apparatus (BAL-TEC/SCD 005).

IV.3. Results and discussion

IV.3.1. Leaching behaviour test

Leaching compliance tests (TCLPs) have identified hazardous characteristics of the waste, especially with regard to mercury content. The concentration of mercury in leachate is almost double the maximum limit permitted by universal treatment standards for this waste (40 CFR 268.48). In contrast, the concentration of mercury in leachates of solidified geopolymer mixtures is well below the standard limit, even for mixtures containing a high percentage of glass waste. For blank mixtures (without glass waste) and those with only 5% glass waste, the mercury concentration is below the limit of analytical determination. This indicates the effectiveness of the use of geopolymers in immobilizing mercury.

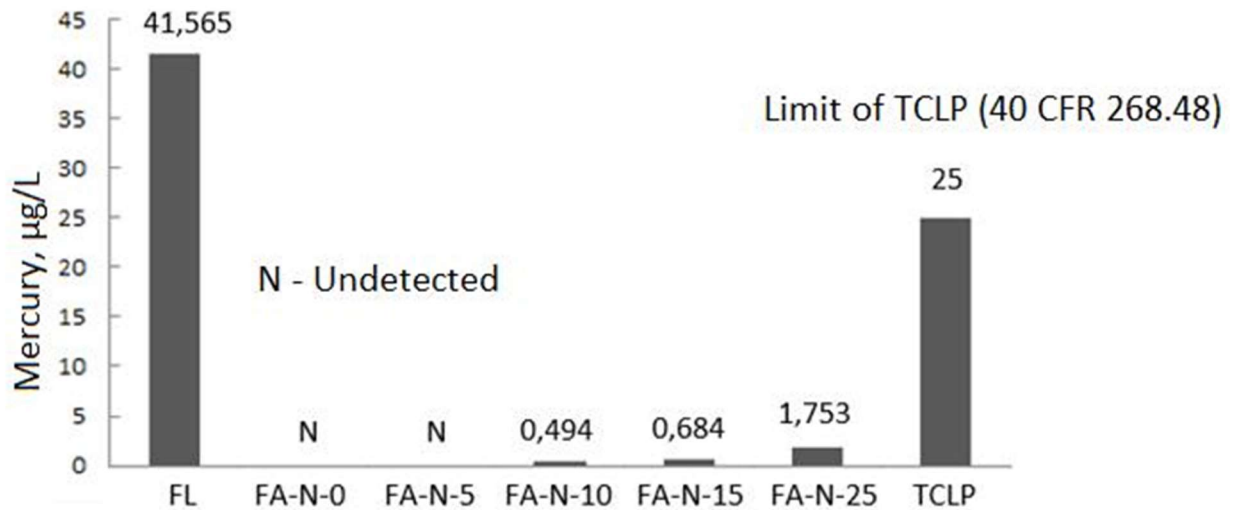


Figure 20. TCLP leaching test results.

All these results suggest a very good potential of geopolymers to immobilize mercury, which is the hazardous component of this waste.

IV.3.2. Compressive strength test

The results of the compressive strength tests for the five geopolymer assortments, shown in Figure 21, show that adding glass waste improves mechanical properties. Although performance decreases with increasing amount of glass, the decrease is not significant. This suggests that glass waste is active in geopolymerization processes.

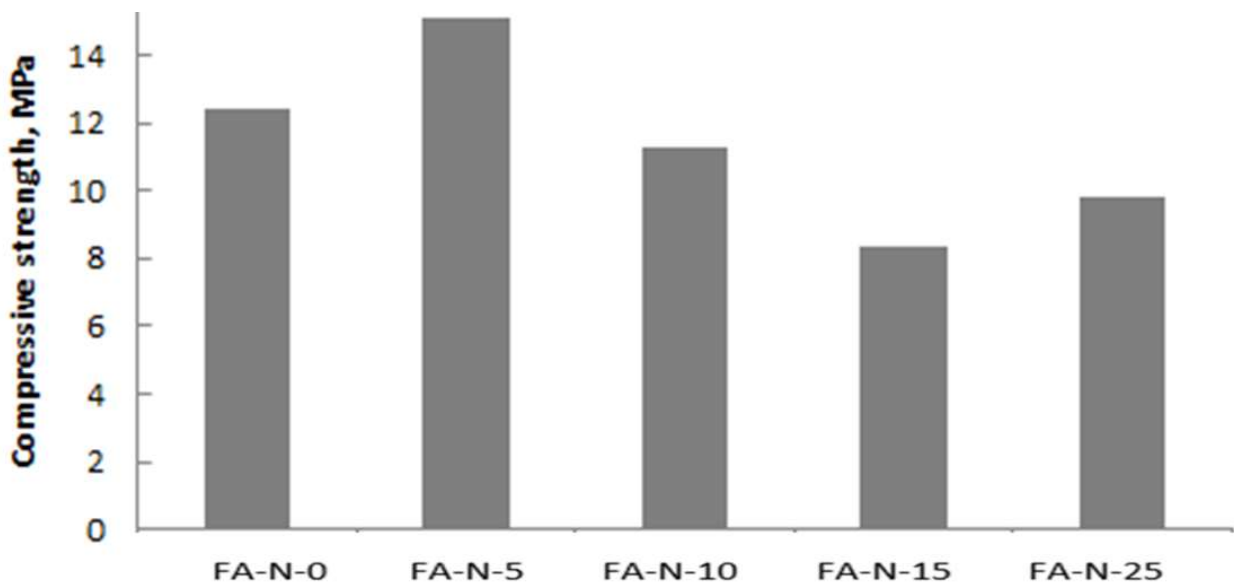
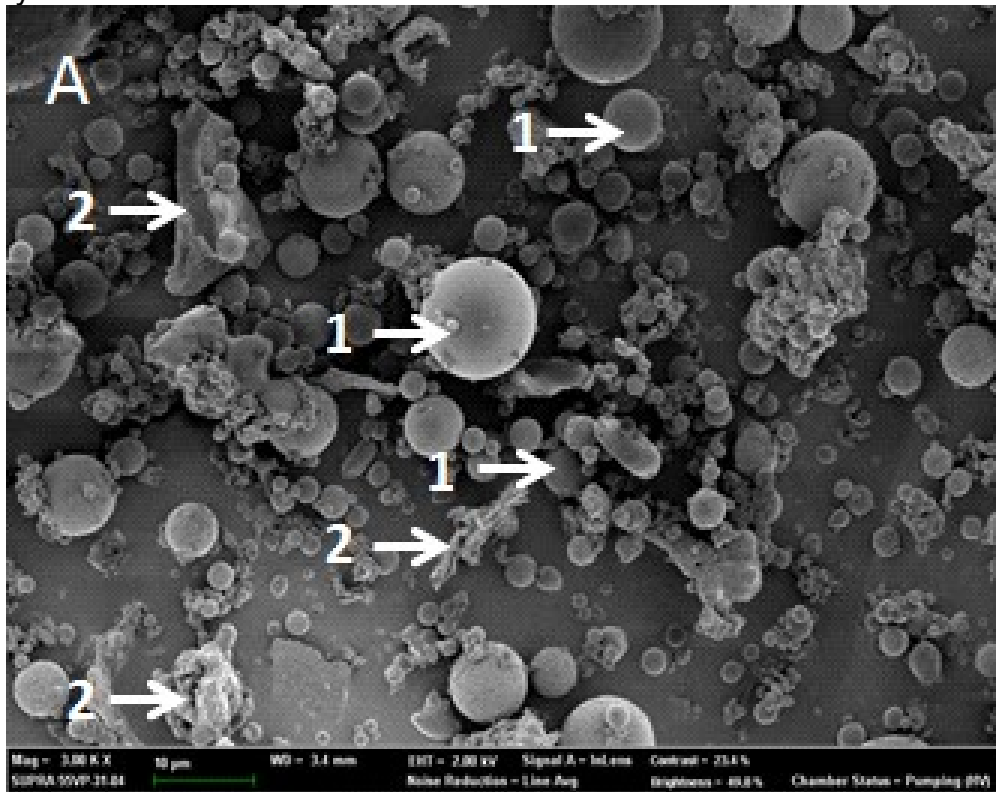


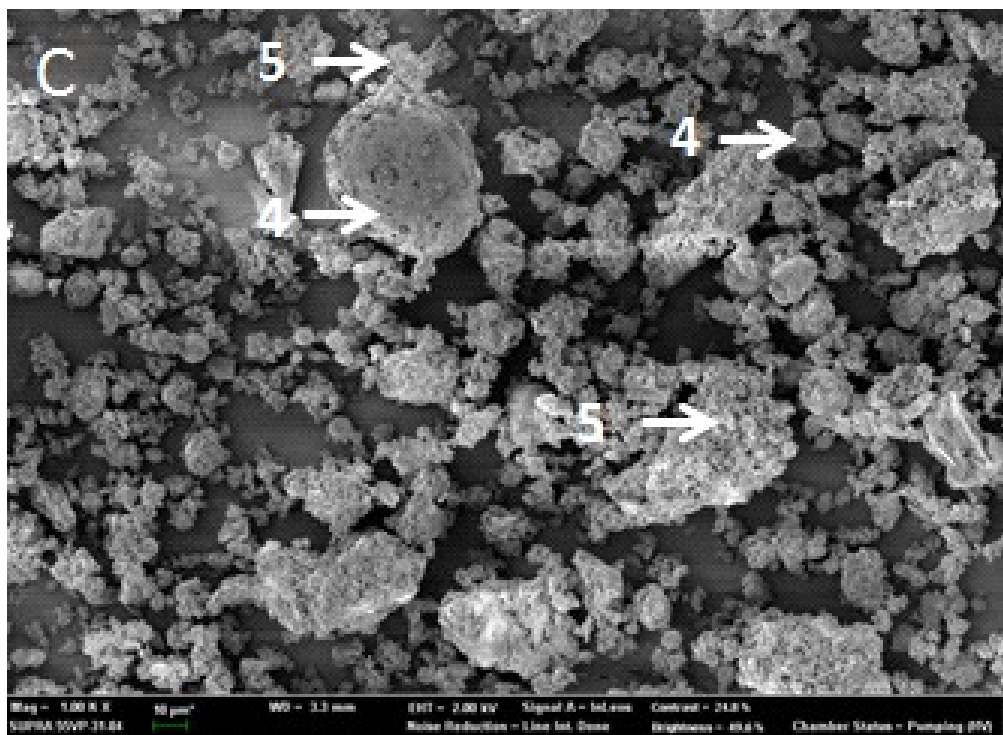
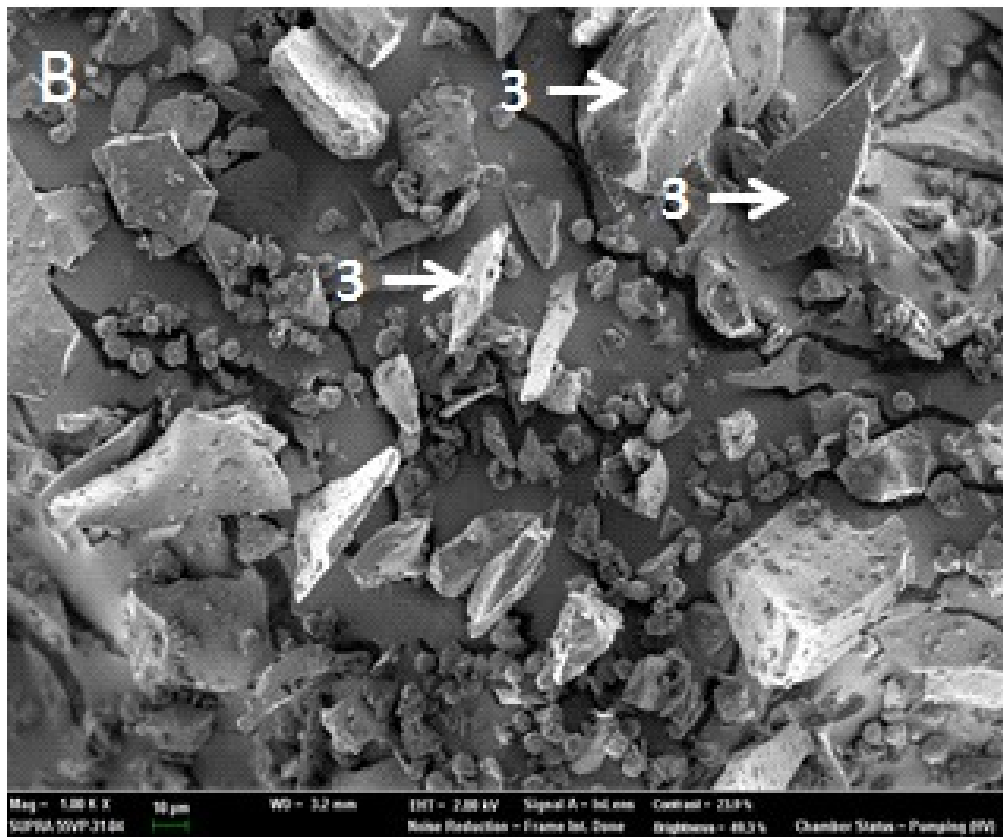
Figure 21. The influence of glass addition on the compressive strength of geopolymers.

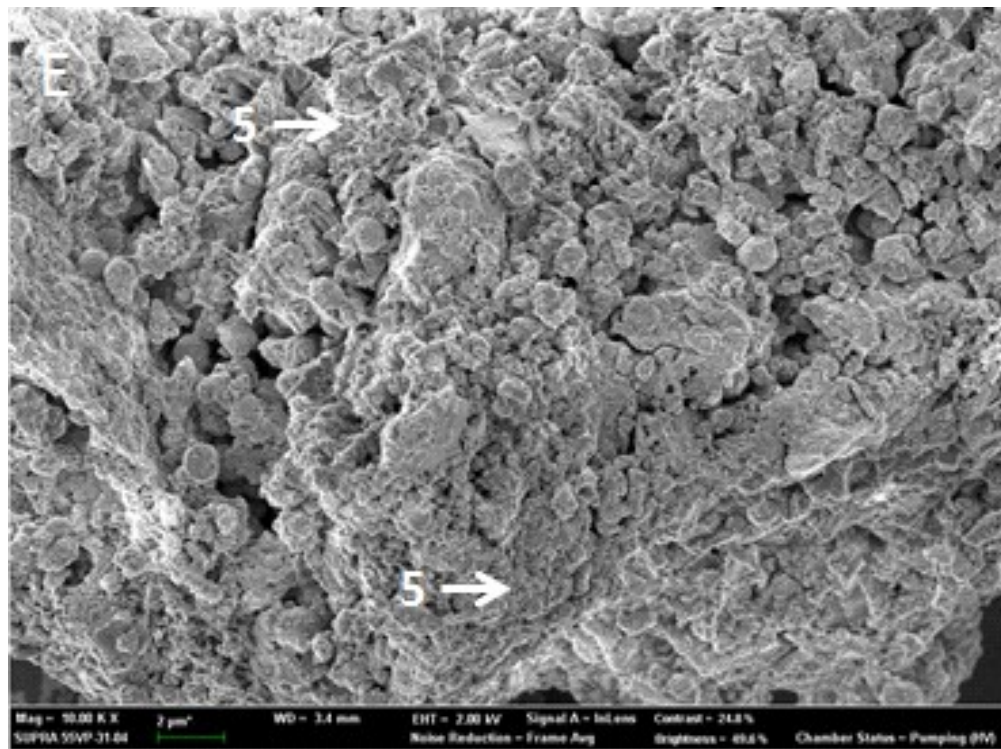
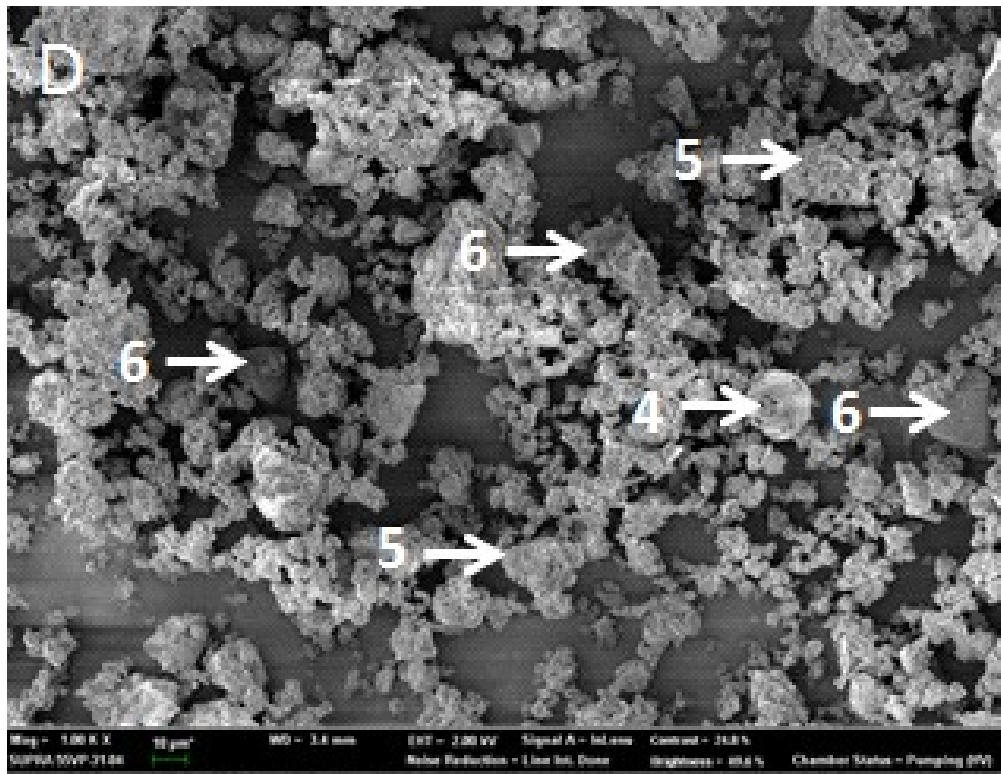
Activation of glass waste powder leads to the formation of a sodium silicate gel, which increases the strength of the geopolymer after hardening. However, adding a higher proportion of glass waste powder to the mixture disrupts the molar $\text{SiO}_2/\text{Al}_2\text{O}_3$ ratio, due to the low alumina content in glass waste. This can lead to the formation of a larger amount of sodium silicate gel at the expense of sodium aluminosilicate gel. In addition, changing the molar ratio $\text{M}_2\text{O}/\text{SiO}_2$ by adding an increasing amount of glass waste leads to a decrease in this ratio in the sodium silicate gel formed, which leads to a decrease in the mechanical properties of the gel and, ultimately, the geopolymer.

IV.3.3. Morphological and structural characterization

The results suggest that both the leaching and mechanical behaviour of geopolymers are significantly influenced by their mineralogical and microstructural characteristics as well as the initial characteristics of the raw materials. Light heat plant ash particles are mainly compacted spheres of various sizes, and glass waste powder exhibits a heterogeneous distribution of irregularly shaped and smooth particles. Compared to materials that have not reacted, activated mixtures highlight the specific morphology of geopolymers and the presence of light ash that has reacted partially or not at all, as well as glass waste particles. These observations indicate a moderate degree of geopolymerisation of the mixture.







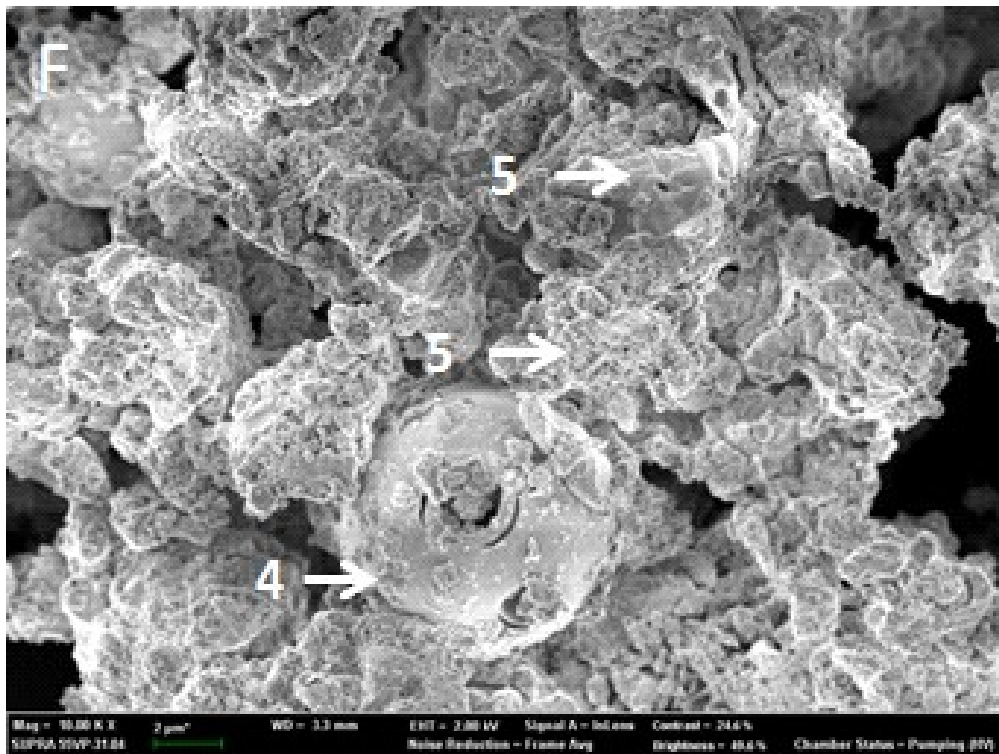


Figure 22. Electronic micrographs of raw materials and two geopolymer mixtures: (A) light ash; (B) glass waste; (C and E) mixture FA-N-0; (D and F) mixture FA-N-10.

Micrographs suggest that the FA-N-10 mixture reacted moderately, with the presence of glass waste particles that did not. These particles have a smooth surface, indicating poor adhesion to the geopolymer matrix, which leads to a decrease in the mechanical strength of the geopolymer. Compared to the FA-N-0 mixture, the FA-N-10 mixture appears to have a continuous solidified gel covering some relatively large portions of the precipitated material, due to the formation of a large amount of sodium silicate gel during activation of the glass waste powder. However, there are some relatively large gaps between these covered areas, which could be attributed to poor adhesion between the geopolymer matrix and the smooth surface of glass waste particles.

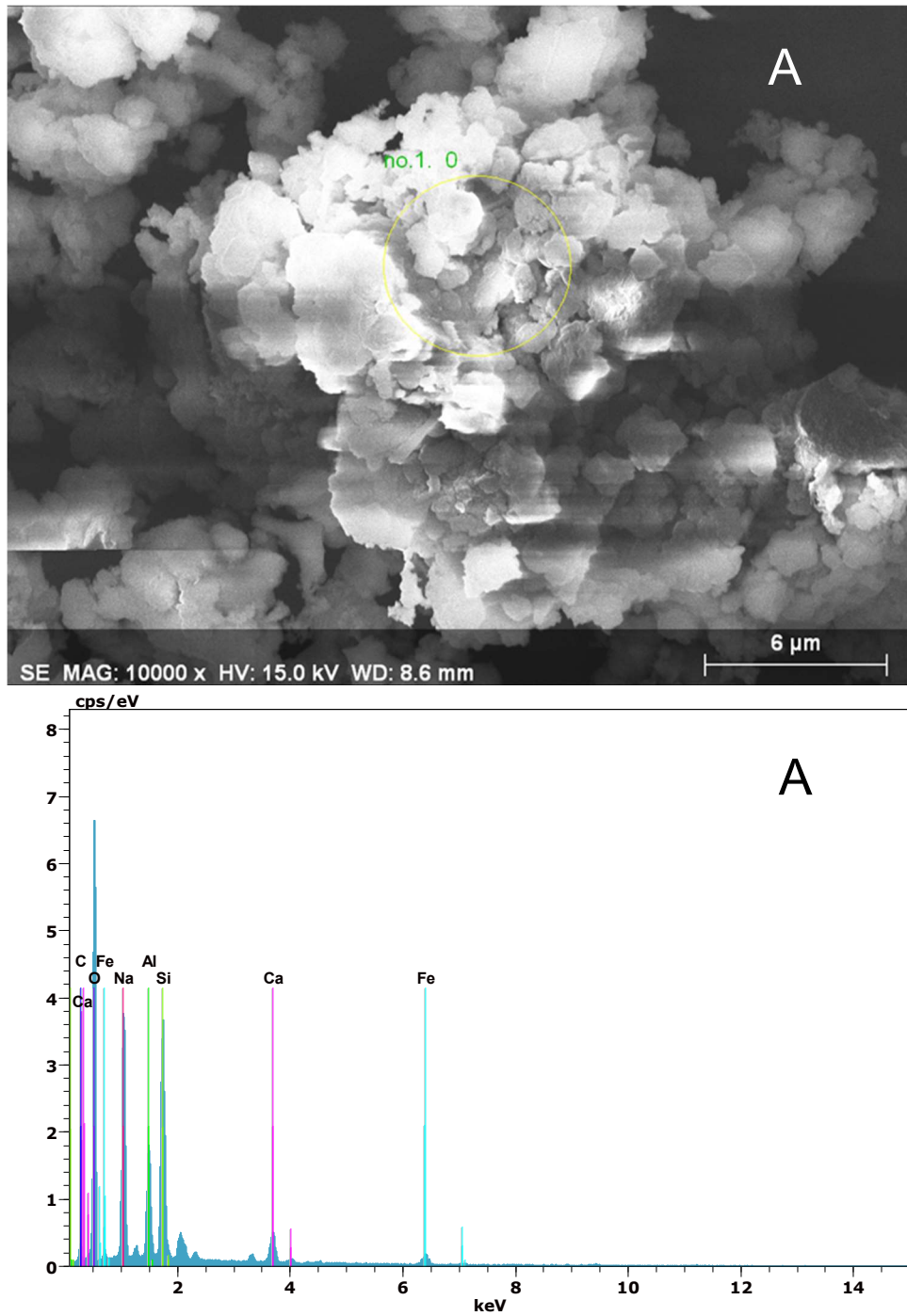


Figure 23. Micrographs and EDX spectra of FA-N-0 geopolymer

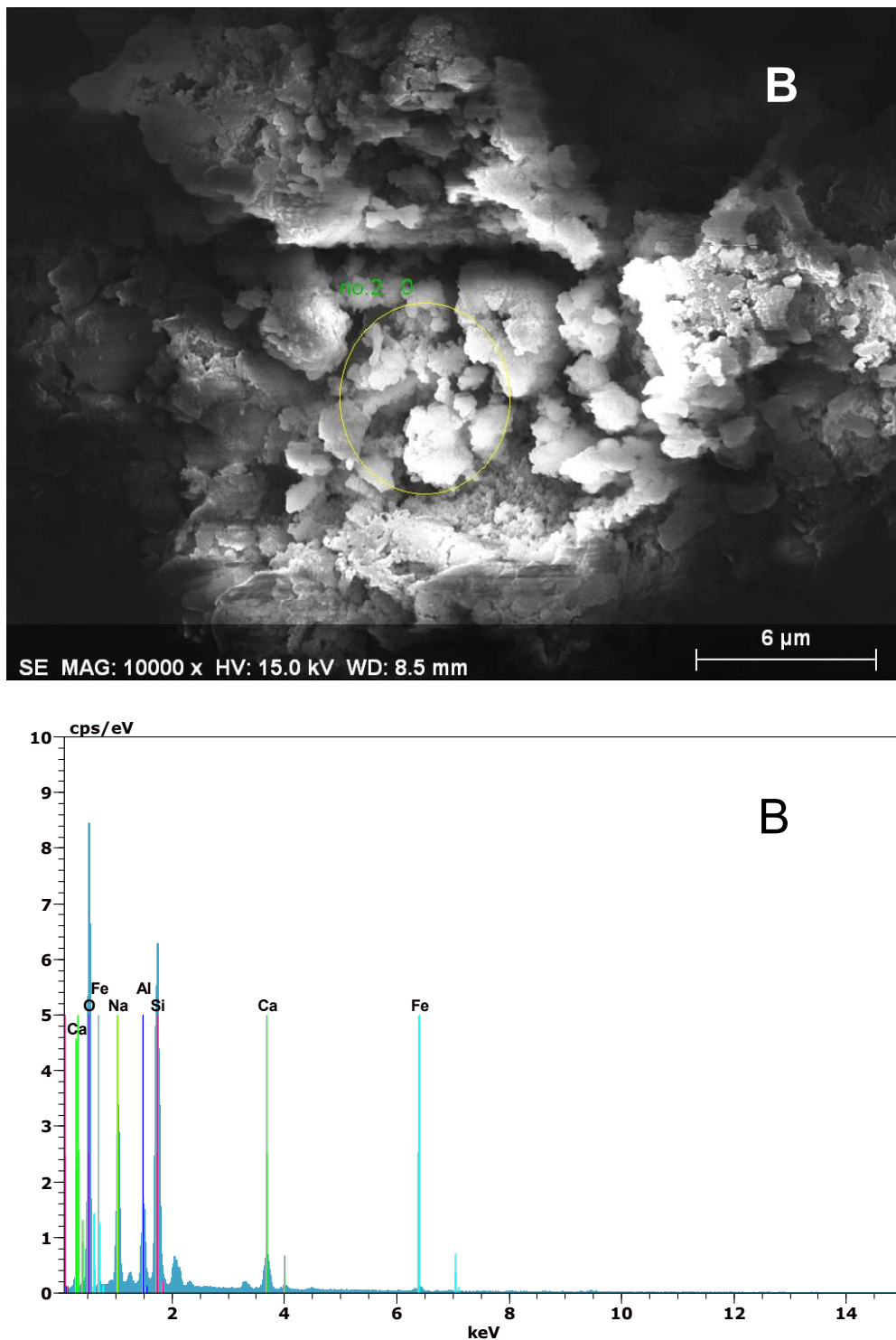
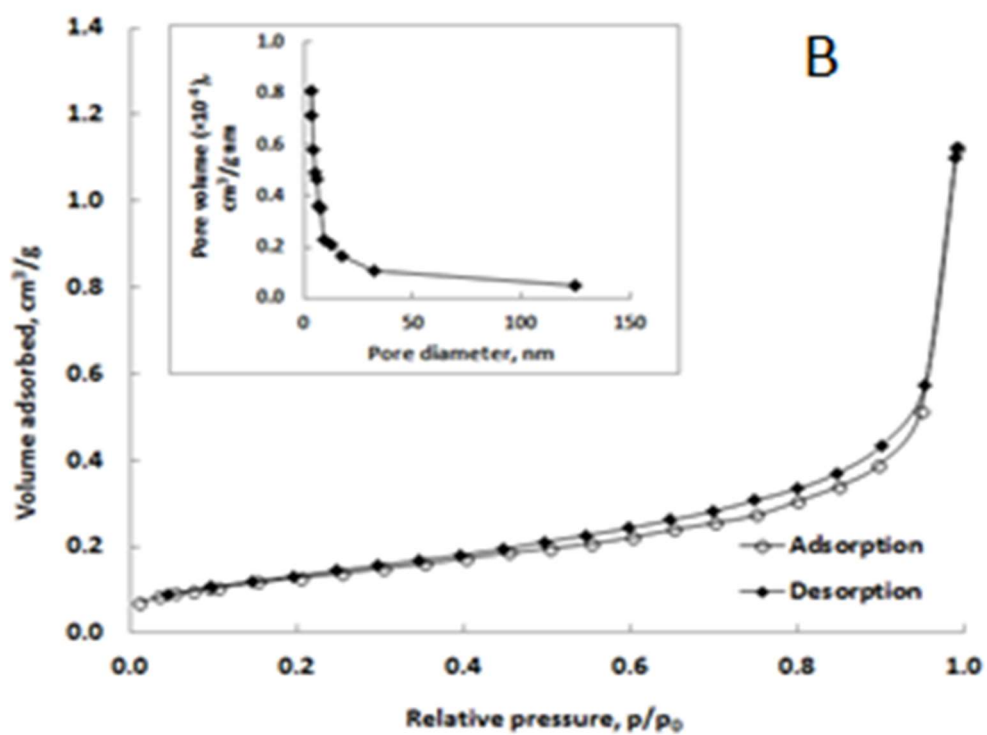
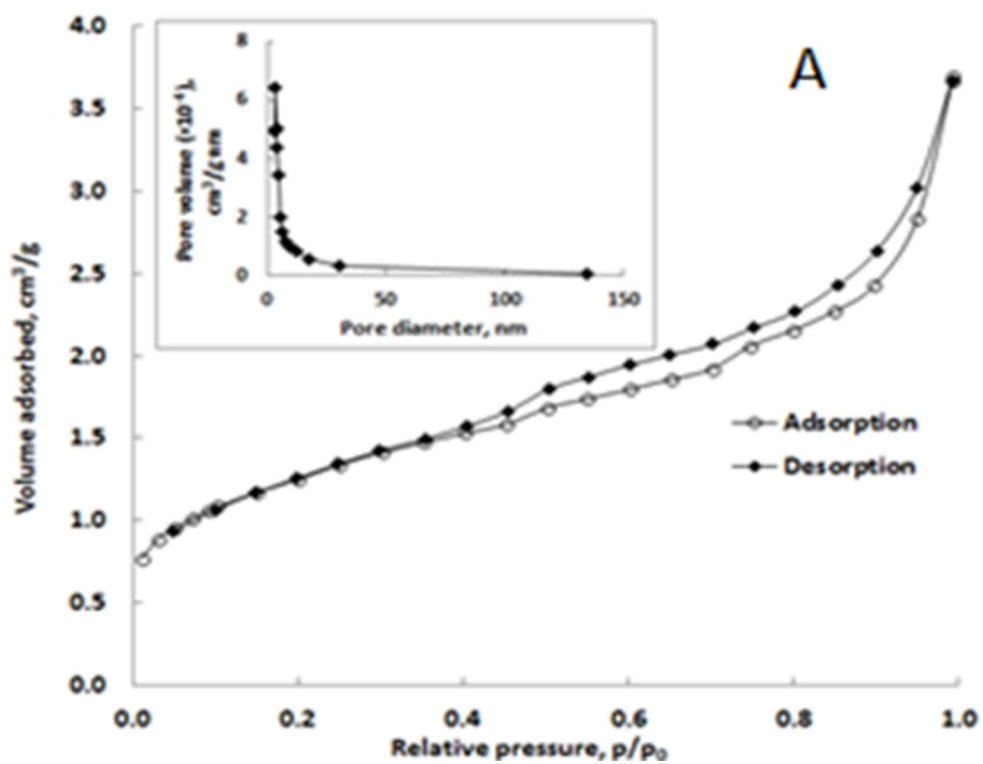


Figure 24. Micrographs and EDX spectra of FA-N-10 geopolymer

EDX analysis of FA-N-0 and FA-N-10 geopolymers (Figure 23 and Figure 24) yields a Si/Al molar ratio of 2.14 for FA-N-0 and 3.26 for FA-N-10, as well as a Na/Al molar ratio of 1.17 for FA-N-0 and 1.34 for FA-N-10. Alkalinely activated materials with a molar Si/Al ratio between 1-3 and a molar Na/Al ratio close to the unit have a geopolymer-specific aluminosilicate structure consisting mainly of gels of the sodium aluminosilicate hydrate (N-A-S-H) type gels. High Si/Al ratio values are associated with the unreacted vitreous fraction of the alkali activated mixture, which forms network defects that have a negative effect on its mechanical properties. These results are consistent with those obtained by SEM analysis and compressive strength tests.



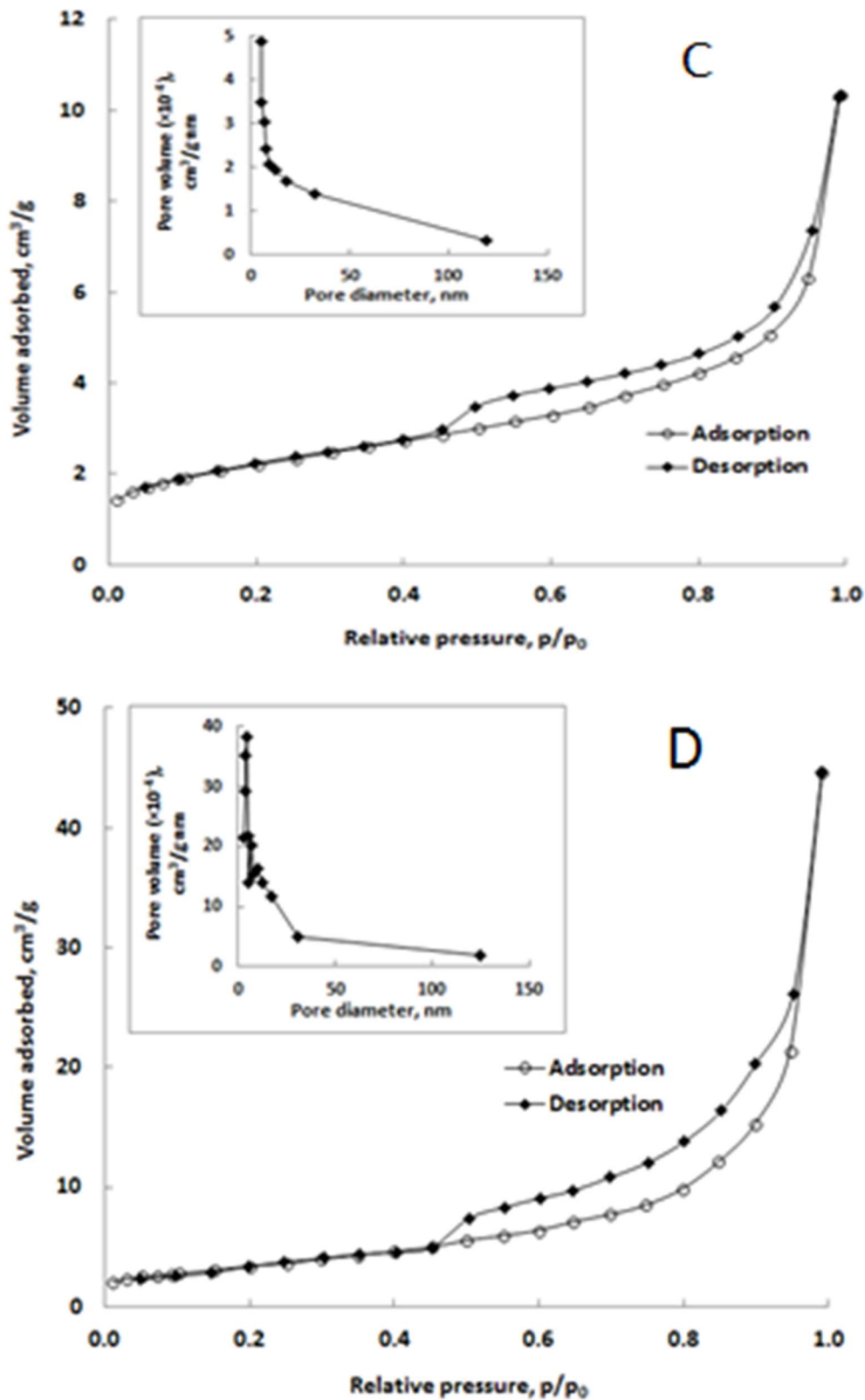


Figure 25. Nitrogen adsorption-desorption isotherms and pore size distribution of both starting materials and geopolymers: (A) light ash; (B) glass waste; (C) mixture FA-N-0; (D) mixture FA-N-10.

Nitrogen adsorption-desorption isotherms for raw materials and geopolymers revealed information about the pore structure. These isotherms can be type II (b), with a type H3 hysteresis loop, typical of mesoporous materials. Most pores in all materials have a diameter of about 3.8 nm, with a tendency to expand to higher values in the case of FA-N-10. The total pore volume for the FA-N-0 mixture is 1.403×10^{-2} cm³/g, while for the

FA-N-10 mixture it is $7.459 \times 10^{-2} \text{ cm}^3/\text{g}$. The BET surface area for the FA-N-0 mixture is $7,834 \text{ m}^2/\text{g}$, while for the FA-N-10 mixture it is $12,55 \text{ m}^2/\text{g}$. These results indicate a significant difference between the two geopolymer systems in terms of their microstructural characteristics, supporting the results obtained from compressive strength tests and SEM analysis.

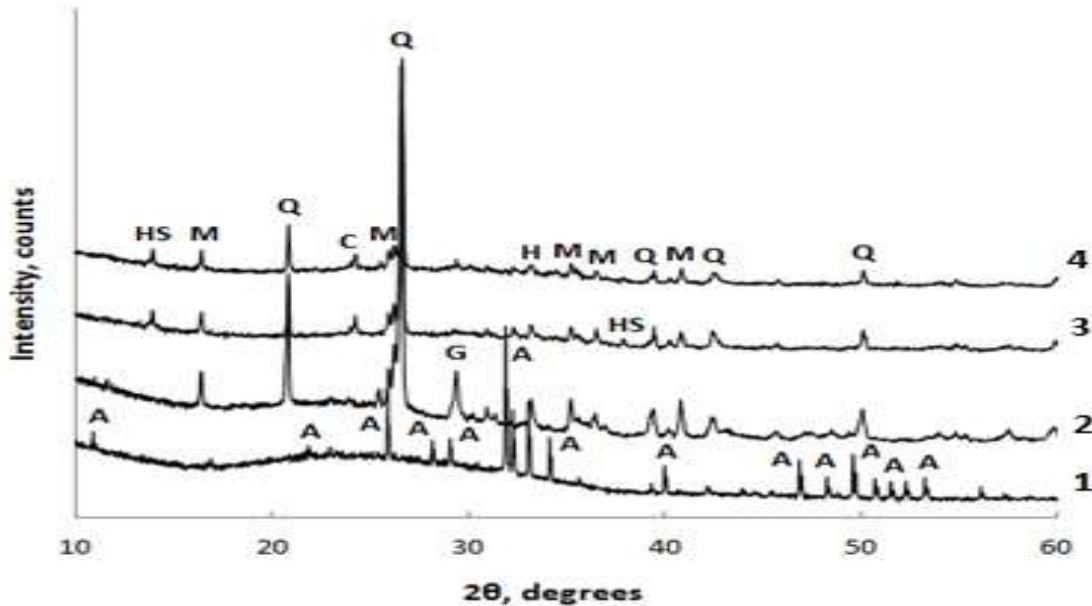


Figure 26. XRD spectra of raw materials and geopolymers; 1. glass waste, 2. thermal power plant ash, 3. mixture FA-N-0; (D) mixture FA-N-10, Q = quartz; M = mullite, H = hematite, G = gypsum; A = hydroxyapatite; HS = hydroxysodalite; C = cancrinite

XRD analysis showed that the raw materials consist mainly of glass phase with a few minor crystalline phases, such as quartz, mullite, hematite and gypsum for light ash and hydroxyapatite for glass waste. Geopolymers have a weakly crystalline structure, associated with the formation of silicate and aluminosilicate gels. Comparing the spectra of geopolymers with those of raw materials, it is observed that the crystal phases initially present were not greatly altered during activation reactions. In the two activated systems, two other crystalline phases were identified, namely zeolites, hydroxysodalite and cancrinite.

IV.4. Partial conclusions

The results of the study show that geopolymers obtained from thermal power plant ash and glass waste can effectively immobilize mercury. The addition of glass waste influences the mechanical performance and microstructure of geopolymers. An adequate amount of glass waste can improve the mechanical performance and immobilizing capacity of mercury.

Chapter V. Preparation of one-part geopolymers based on light ash and addition of red mud using alternative solid activators based on glass waste

V.1. Specific objectives

The main objectives of this chapter were:

- ✓ Synthesis of a new class of solid activators based on waste glass by alkaline fusion. The optimization of the alkaline fusion process is considered;

- ✓ Characterization of solid activators synthesized by mineralogical, morphological and spectroscopic analysis;
- ✓ Preparation of geopolymer cements using the best assortment of solid activators;
- ✓ Preparation of several assortments of geopolymers using geopolymer cements with solid activator, followed by testing their compressive strength;
- ✓ Characterization of geopolymers for which the best mechanical performances have been recorded by mineralogical, morphological and spectroscopic analysis.

V.2. Materials and methods

V.2.1. Materials

Glass waste from cathode ray tubes (CRTs) was ground to a particle size below 75 μm . The oxide composition of CRT glass, light ash and red mud is shown in Table 13. Sodium hydroxide was used to synthesize the solid alkaline activator. Light ash, supplied by a coal-fired power plant, and red mud, a bauxite residue supplied by an alumina refining plant, were also used as raw materials.

V.2.2. Synthesis of solid alkaline activators

CRT powder and NaOH granules were mixed dry in three different NaOH:CRT mass ratios until homogeneous mixtures were obtained. The resulting solid alkaline activator assortments are coded and shown in Table 14.

CRT-NaOH mixtures were stored for 2 hours in an electric furnace at temperatures of 500, 600 and 700 $^{\circ}\text{C}$ (alkaline fusion). At the end of alkaline fusion, the synthesized solid alkaline activators were cooled and finely ground.

V.2.3. Preparation of one-part cements based on red mud and light ash

One-part cements were prepared by mixing light ash, red mud and solid activator. After 28 days of curing, they were tested for compressive strength and analyzed morphologically and spectroscopically. The cement was mixed with water at a water/cement mass ratio of 0.5, poured into formwork and heat-treated at 80 $^{\circ}\text{C}$ for 28 days.

V.2.4. Characterisation and testing of synthesized solid alkaline activators and prepared one-part geopolymers

Solid alkaline activators were tested for water solubility and their Si and Na content determined. They were also characterized by spectroscopic and mineralogical analysis. One-part geopolymers have been morphologically and spectroscopically characterized and tested for compressive strength. Methods used include flamphotometry, spectrometry, Fourier transform infrared spectroscopy (FT-IR), X-ray photoelectron spectroscopy (XPS), magic angle nuclear magnetic resonance (MAS-NMR), X-ray diffractometry (XRD), and scanning electron microscopy coupled with energy dispersion X-ray spectroscopy (SEM/EDX).

V.3. Results and discussions

V.3.1. Water solubility

The water solubility of solid activators is essential for the manufacture of one-part geopolymers. These activators must provide the alkali needed to attack the T-O-T (T: Si or Al) bonds in the precursors, forming T-OH groups that subsequently condense and form gels of aluminosilicates. The solubility of solid activators depends on the conditions of synthesis. Assortments with a NaOH:CRT mass ratio of 2, synthesized at a temperature of 600 $^{\circ}\text{C}$, have the highest solubility. This also corresponds to the lowest water-soluble $\text{SiO}_2/\text{Na}_2\text{O}$ mass ratio, which depends on the synthesis temperature of the solid activators. The synthesis temperature controls the type of sodium silicates formed

and their share in the composition of the activator. Increasing the amount of sodium hydroxide leads to an increase in the percentage of solubilized activator.

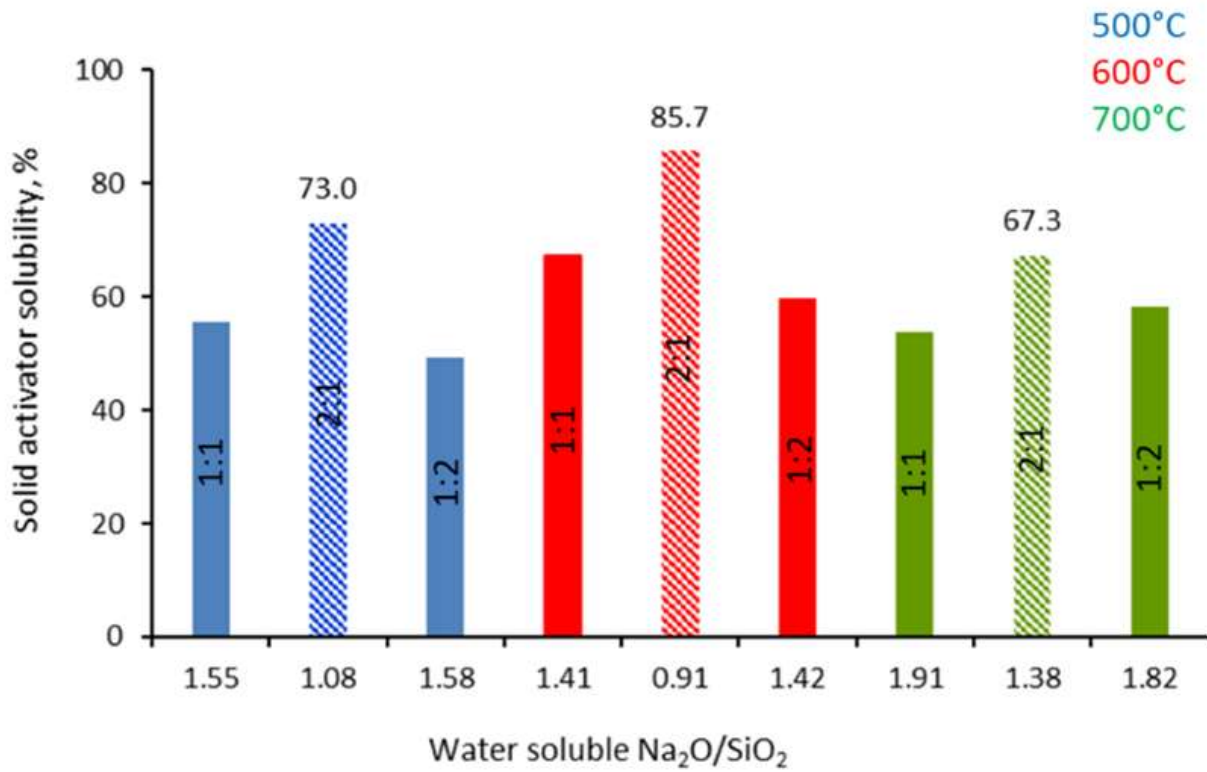


Figure 27. Water solubility of synthesized solid activators.

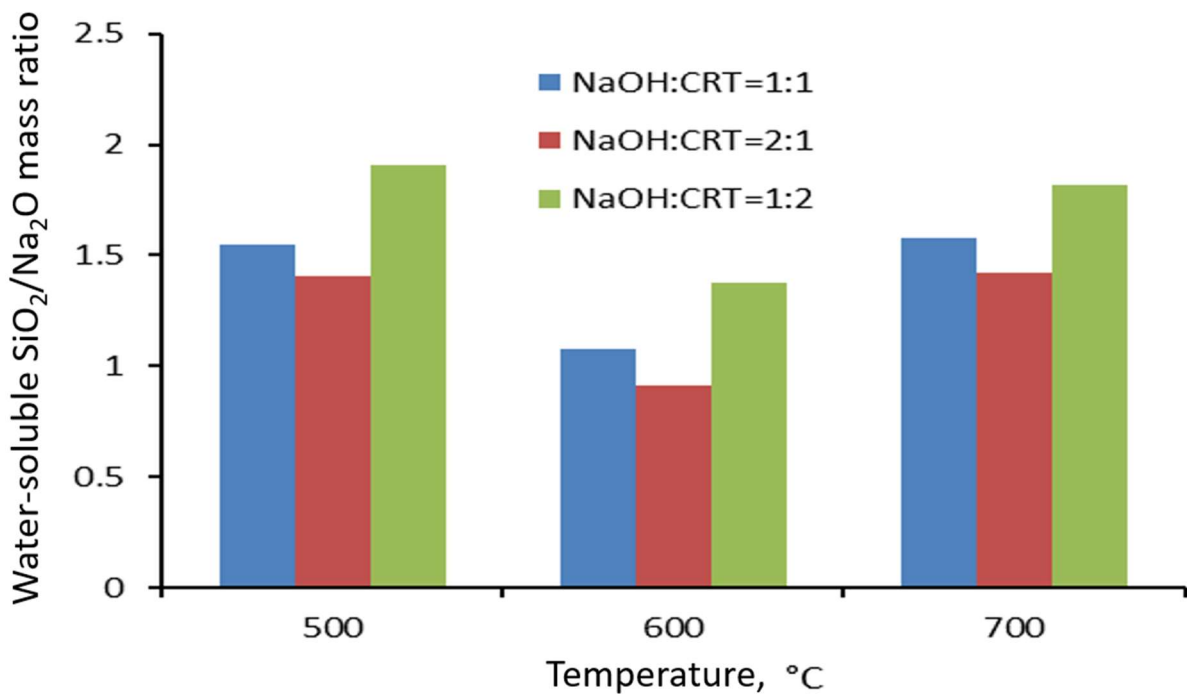


Figure 28. Water-soluble $\text{SiO}_2/\text{Na}_2\text{O}$ mass ratio as a function of alkaline fusion temperature.

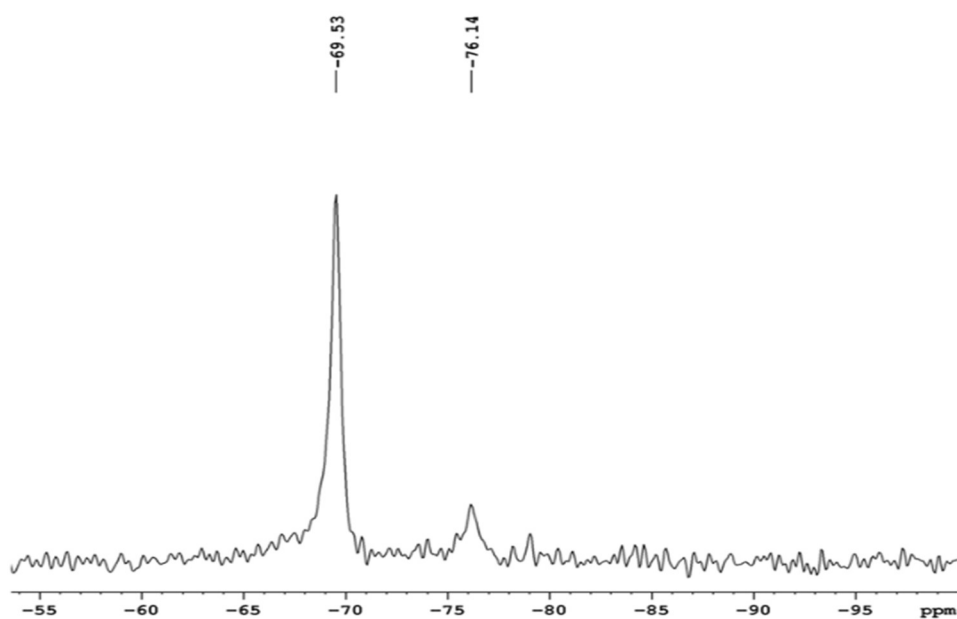
The solubility of solid activators in water is crucial for the manufacture of one-part geopolymers. Solubility depends on the conditions of synthesis, with best results obtained

for a NaOH:CRT mass ratio of 2:1 and a synthesis temperature of 600 °C. This is due to the fact that at this temperature easily soluble sodium silicates are formed in water. At higher temperatures, more complex sodium silicates with lower solubility are formed. Also, part of the sodium hydroxide may remain unreacted or react with other components of the glass, contributing to the alkalinity of the solid activator.

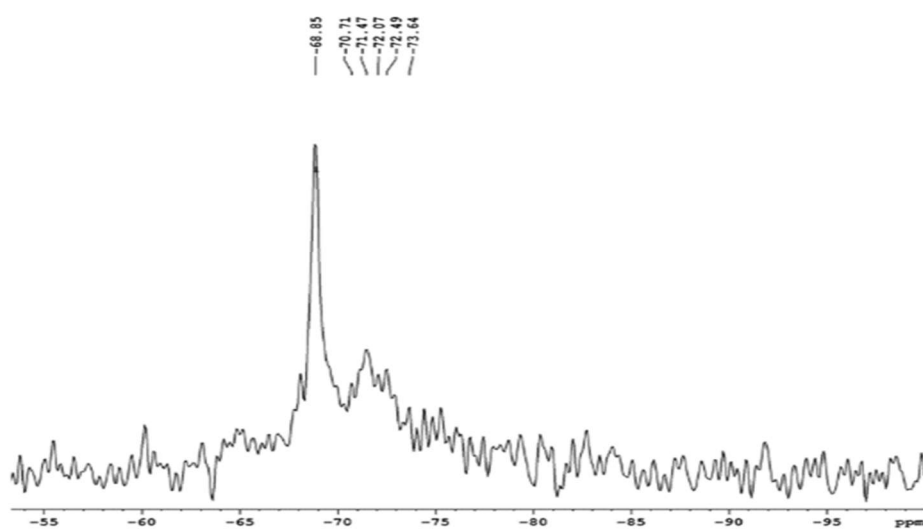
V.3.2. Characterisation of solid activators

V.3.2.1. Assay ^{29}Si MAS-NMR

^{29}Si MAS-NMR measurements showed that the degree of connectivity of SiO_4 tetrahedra in solid activators is influenced by synthesis temperature. For the NaOH:CRT=2:1 600 assortment, the peaks in the spectrum are associated with Q1 units. For the NaOH:CRT=2:1 500 assortment, peaks are associated with units Q1 and Q2. For the NaOH:CRT=2:1 700 assortment, a transition to units Q2 and Q3 is observed. As the proportion of units Q3 and Q4 increases, the connectivity of SiO_4 tetrahedra increases and their reactivity in the activation process decreases.



a.



b.

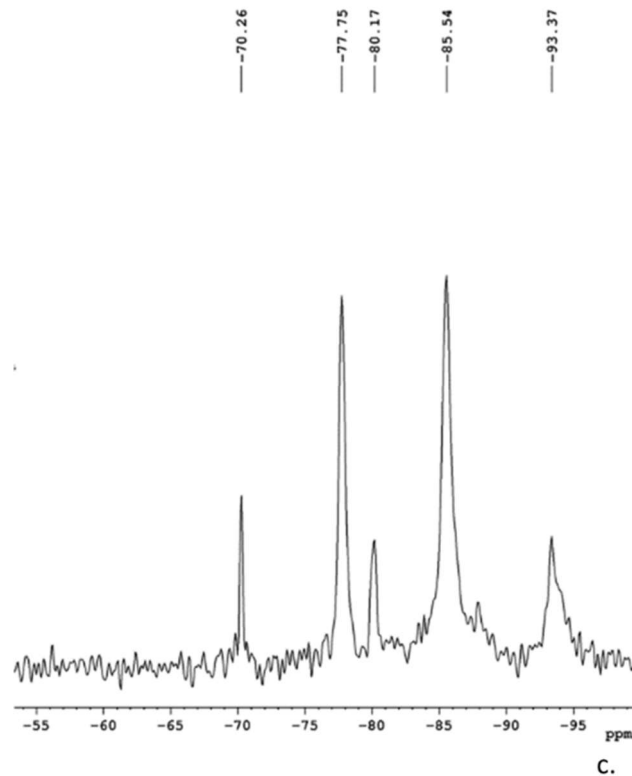


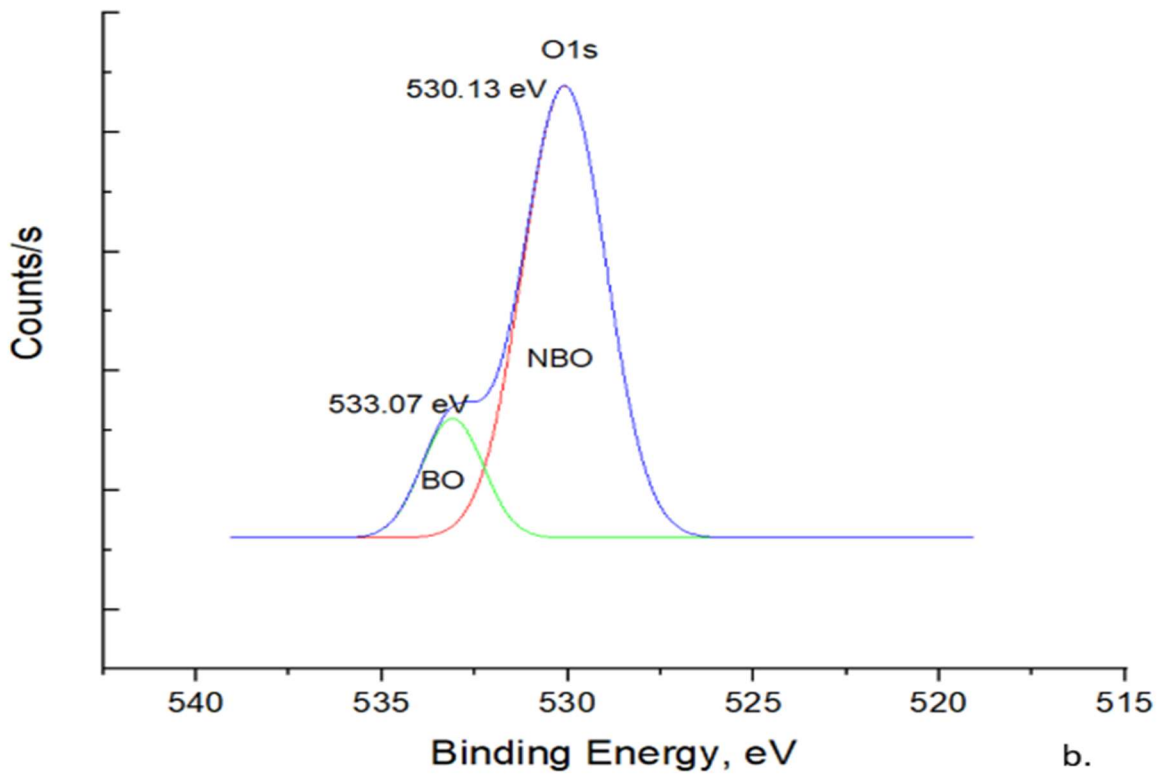
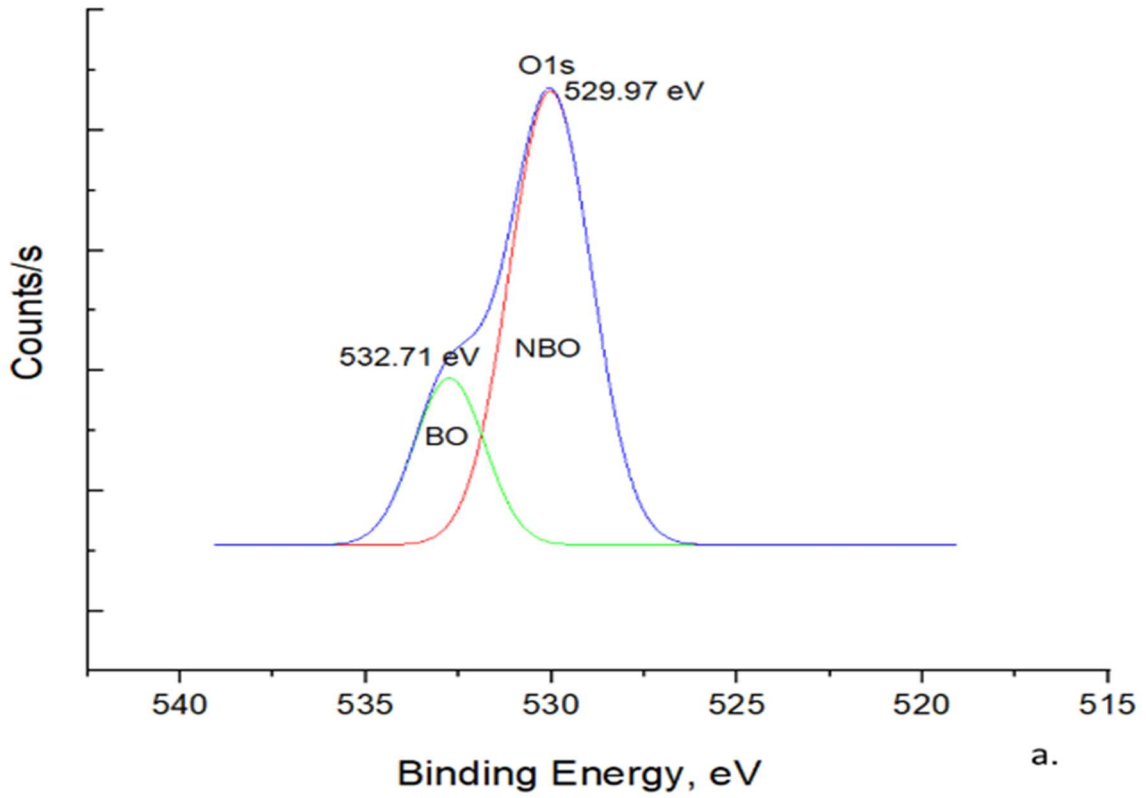
Figure 29. Spectra ^{29}Si MAS-NMR of solid activators: a. NaOH: CRT=2:1 600;

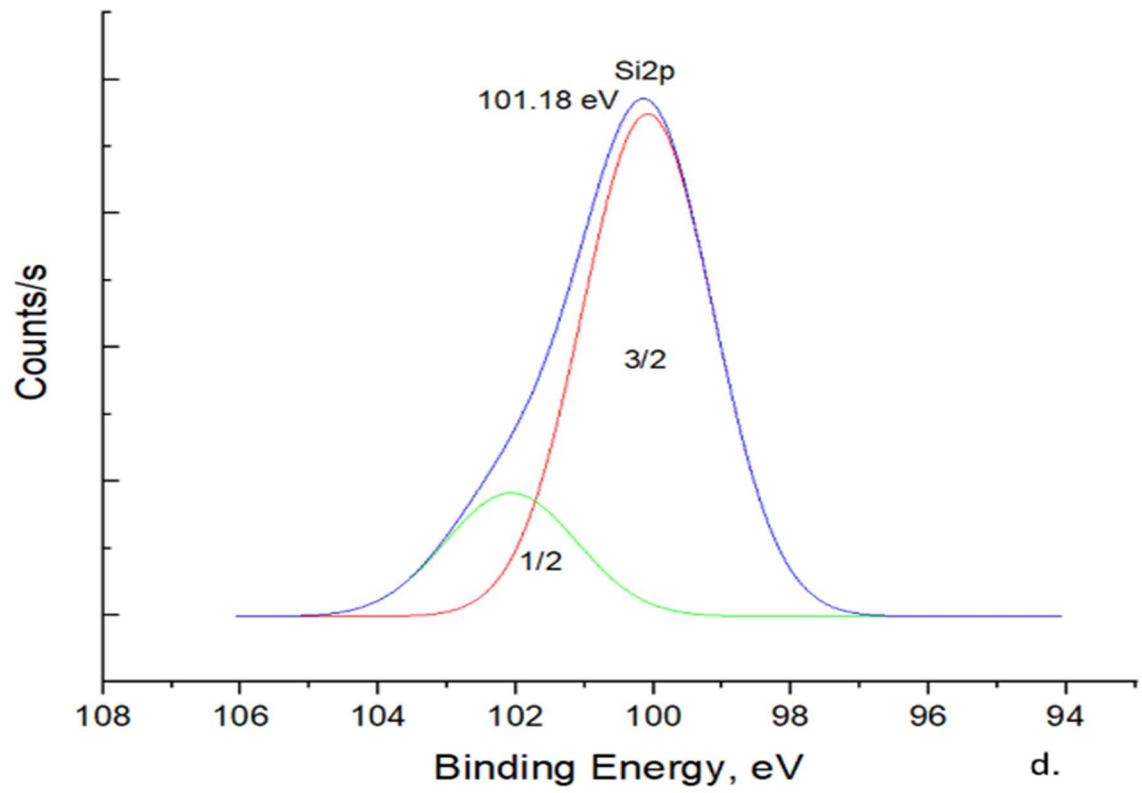
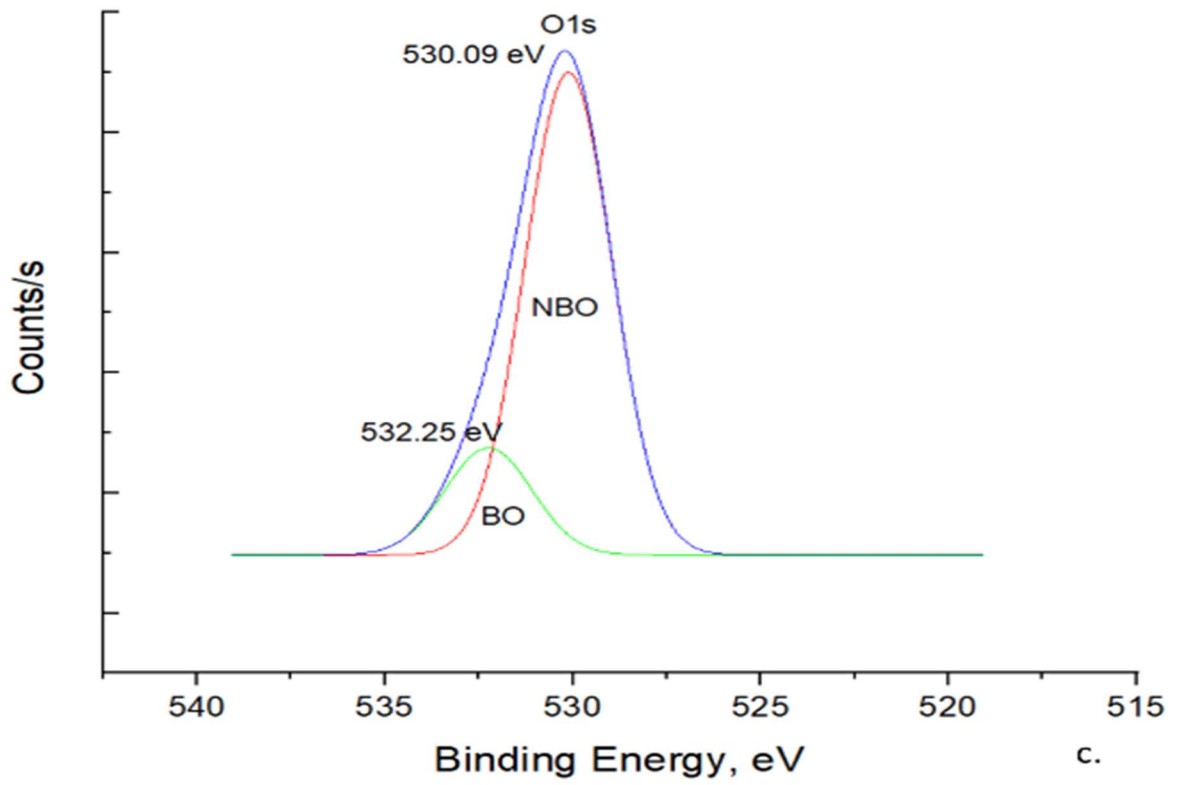
b. NaOH: CRT=2:1 500; c. NaOH: CRT=2:1 700

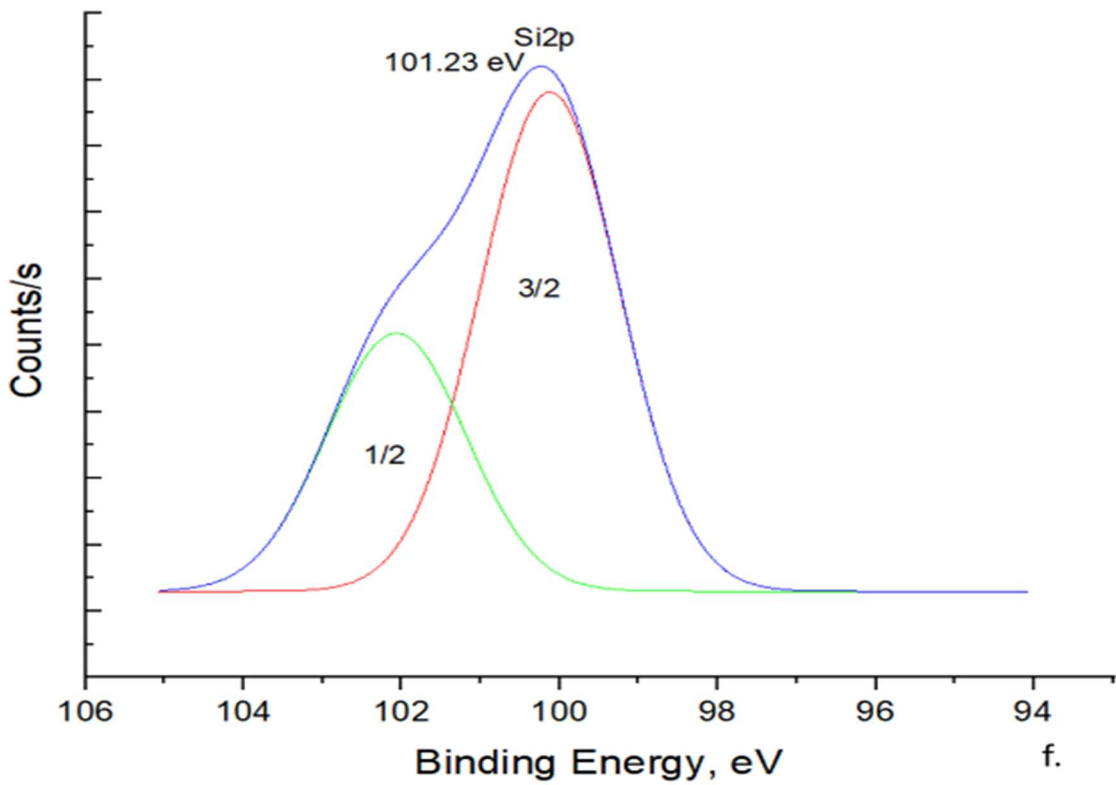
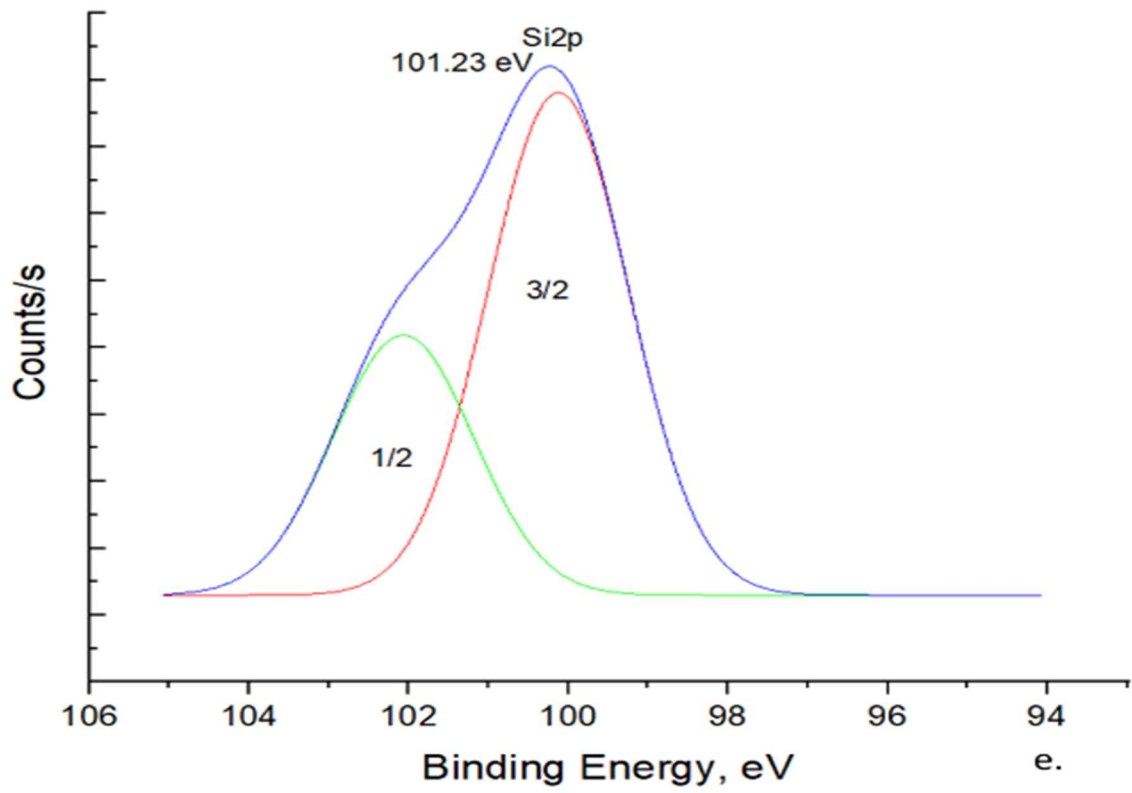
V.3.2.2. Spectroscopie XPS

Spectrele O 1s

In the process of alkaline fusion of CRT glass with NaOH, Na_2O breaks the bonds in the tetrahedral lattice of SiO_4 and introduces a new oxygen atom into the system. This leads to the formation of oxygen atoms bonded to a single silicon atom (unbonded oxygen - NBO: Si-O-), which acquire a negative charge. Sodium ions associate with these negatively charged oxygen atoms. Since bonding oxygen (BO: Si-O-Si) has a weak electron density, a greater amount of energy is required to remove a photoelectron from the O 1s orbital, resulting in higher binding energy. In contrast, NBO has a higher electron density, requiring less energy to remove a photoelectron from the O 1s orbital, resulting in lower binding energy. These observations are supported by O 1s spectra measured by XPS with Gaussian peak deconvolution.







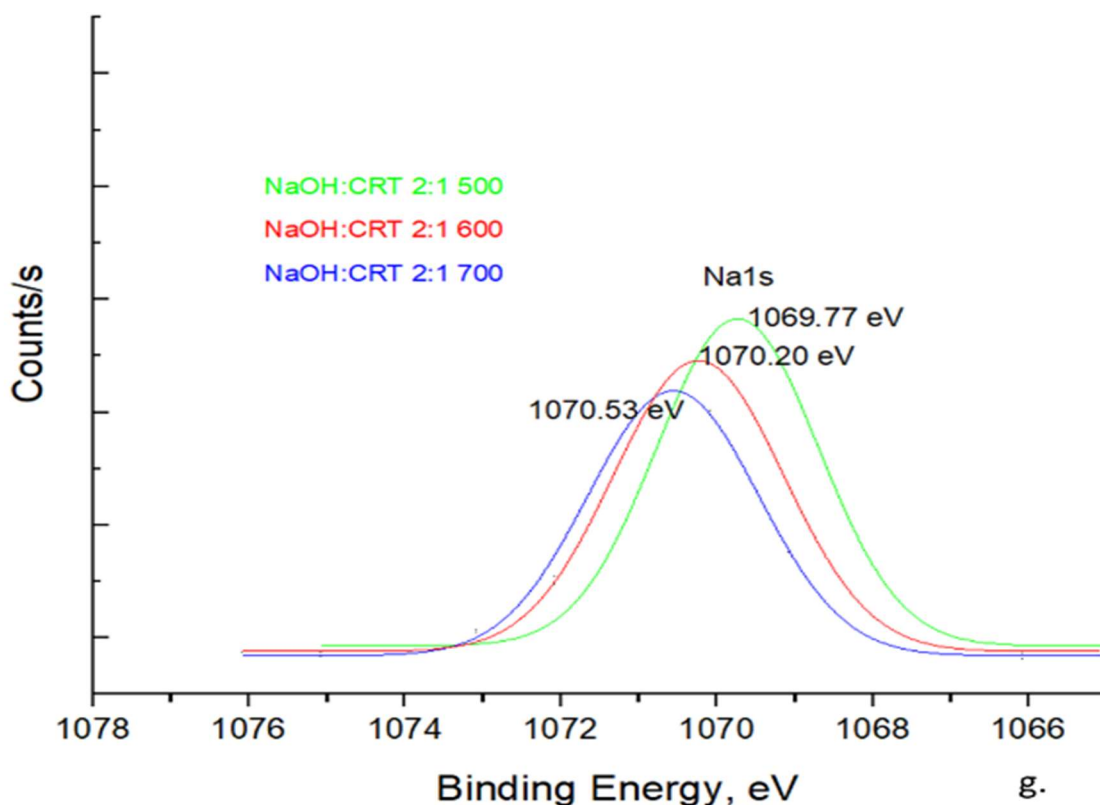


Figure 30. XPS spectre with Gaussian peak deconvolution: a. O 1s for NaOH: CRT 2:1 500; b. O 1s for NaOH: CRT 2:1 600; c. O 1s for NaOH: CRT 2:1 700; d. Si 2p for NaOH: CRT 2:1 500; e. Si 2p for NaOH: CRT 2:1 600; f. Si 2p for NaOH: CRT 2:1 700; g. Na 1s.

The results presented in Figure 30 indicate that the binding energy for BO and NBO shifts towards higher values for the solid activator synthesized at 600°C, compared to the one synthesized at 500°C. This trend does not hold for the activator synthesized at 700°C, where the binding energy is again shifted towards lower values. This behavior can be explained by changes in the electronic density of oxygen atoms depending on the number of silicon atoms they are bound to.

Analyzing the soluble $\text{Na}_2\text{O}/\text{SiO}_2$ ratio of the solid activators, a concordance is observed between the values of this ratio and the results obtained from the O 1s spectra. The decrease in the soluble $\text{Na}_2\text{O}/\text{SiO}_2$ ratio from 1.08 for the assortment of solid activators synthesized at 500°C to 0.91 for the assortment synthesized at 600°C indicates the presence of more silicon atoms in the system. This could lead to a decrease in the electronic density of the oxygen atoms and thus, the binding energy for both BO and NBO is shifted towards higher values.

Similarly, the increase in the $\text{Na}_2\text{O}/\text{SiO}_2$ ratio from 0.91 for the assortment of solid activator synthesized at 600°C to 1.82 for the assortment synthesized at 700°C reflects a decrease in the number of Si atoms in the system. This could also increase the electronic density of the oxygen atoms and thus, change the binding energy for both BO and NBO to lower values.

It appears that the presence of a larger amount of soluble SiO_2 in the system leads to an increase in the NBO fraction at the expense of the BO fraction. Thus, it was established that for the assortment synthesized at 500°C, the BO fraction is 0.27 and the NBO is 0.73, for the assortment synthesized at 600°C the BO fraction is 0.23 and the NBO is 0.77, and for the assortment synthesized at 700°C the BO fraction is 0.25 and the NBO is 0.75.

Spectra Si 2p

The XPS spectra of Si 2p, with the peaks deconvoluted by the Gaussian method, indicate that the binding energy of the Si 2p peak varies similarly to the binding energy of the O 1s peak. The binding energy is shifted towards higher values for the mixture synthesized at 600°C, compared to the one synthesized at 500°C, and is again shifted towards lower values for the mixture synthesized at 700°C. The increase in Na₂O content in the system leads to an increase in the electronic density at the level of the Si cores, which results in the displacement of the binding energy of Si 2p_{3/2} towards lower values.

This behavior suggests that the degree of connectivity of the SiO₄ tetrahedron (Q_n) depends on the number of NBO atoms bound to the central Si atom. As the number of NBO atoms bound to the central Si atom increases, the electron density of the central Si atom increases and, therefore, the binding energy of the Si 2p peak systematically decreases from Q₄ units to Q₀ units. These results are in agreement with those obtained from the analysis of ²⁹Si MAS-NMR, where the assortment of solid activator synthesized at 600°C is characterized by Q₁ units, compared to the other assortments which appear to be mainly characterized by Q₂ and Q₃ units.

Spectra Na 1s

XPS spectra of Na 1s with peaks deconvoluted by the Gaussian method are shown in Figure 30 g. As can be seen, although there is a small displacement of the binding energy with increasing synthesis temperature of solid activators, it can still be stated that sodium exists in a single bond configuration.

V.3.2.3. FT-IR analysis

The FT-IR spectra of the solid activators highlight various absorption bands that correspond to different types of vibrations of chemical bonds. These include symmetric stretching vibrations of Si-O(Na) bonds at 877.54 cm⁻¹, asymmetric deformation vibrations of (H)O-Si-O(Na) and (H)O-Si-O(H) bonds at 621.03 cm⁻¹ and 754.11 cm⁻¹, respectively. Also present are asymmetric stretching vibrations of Si-O-Si bonds at 1026.05 cm⁻¹ and Si-O(Na) at 1161.06 cm⁻¹. The accentuated absorption band at 1427.21 cm⁻¹ is attributed to the stretching vibration of O-C-O bonds in Na₂CO₃, and the absorption bands at 1774.38 cm⁻¹ and 2983.65 cm⁻¹ are attributed to the bending vibrations of H-O-H molecules and the stretching vibrations of O-H, respectively.

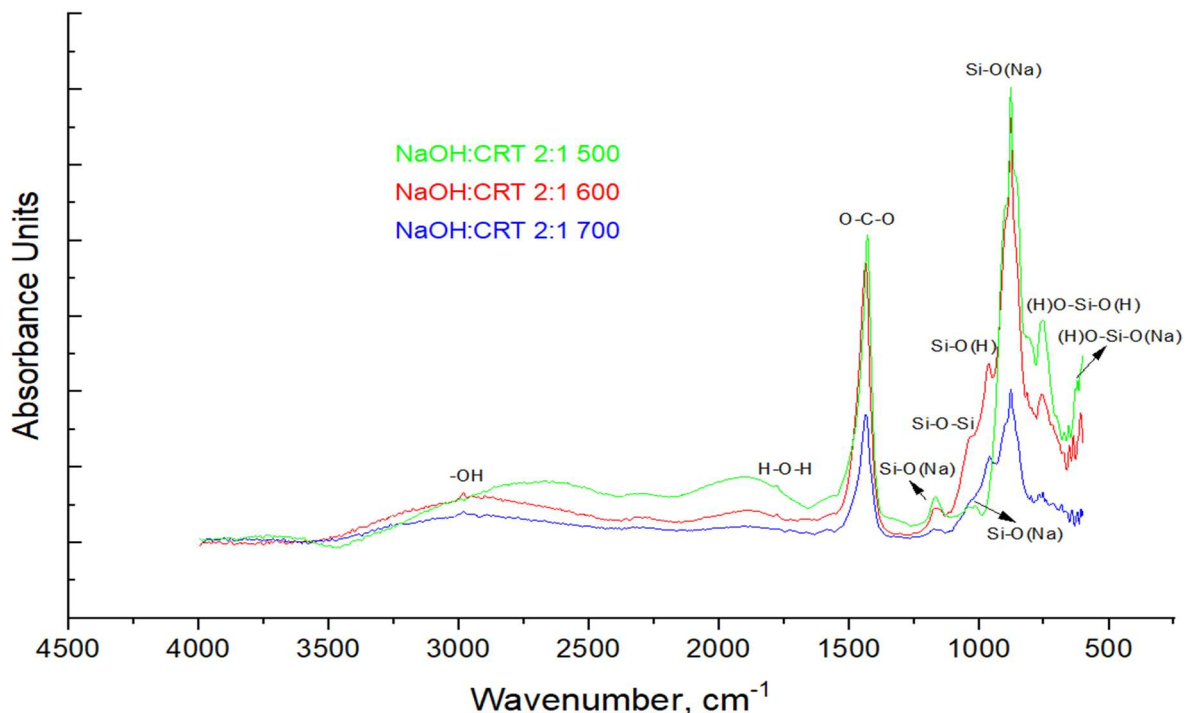
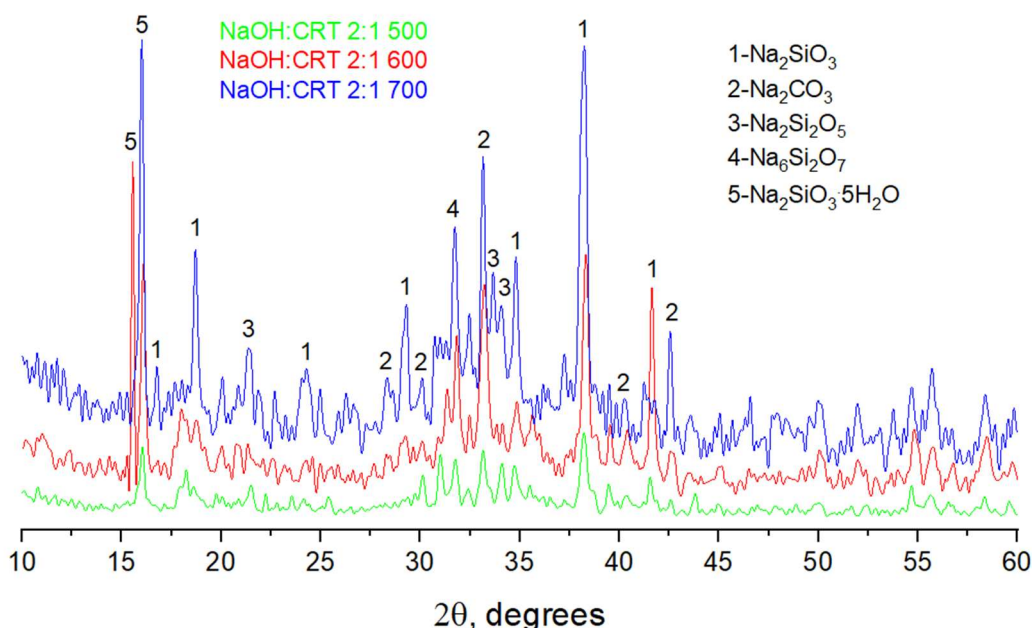


Figure 31. FT-IR spectra of solid activators.

FT-IR analysis results are consistent with those obtained by MAS-NMR and XPS analyses. The absorption band at approximately 880 cm^{-1} can be assigned to Q1 units (Si-O-3NBO), and that at approximately 958 cm^{-1} can be assigned to Q2 units (Si-O-2NBO). The wide signal in the range $1020\text{-}1040\text{ cm}^{-1}$ may include two overlapping peaks, attributed to siloxan Si-O-Si bond and Q3 (Si-O-1NBO) units. These interpretations are supported by the literature (Gaggiano et al., 2013; Vinai and Soutsos, 2018).

V.3.2.4. XRD analysis

**Figure 32.** XRD spectra of solid activators.

XRD diffraction spectra of solid activators show low and dispersed bands, indicating an unordered crystal structure, possibly due to the formation of a silica-rich gel. A wide band observed in the range of $30\text{-}35\text{ }2\theta$ may be associated with unreacted glass or the formation of silicon-rich polymers. Sharp bands indicate the presence of crystal phase of sodium metasilicate (Na_2SiO_3), sodium silicate pentahydrate ($\text{Na}_2\text{SiO}_3 \cdot 5\text{H}_2\text{O}$) and sodium carbonate (Na_2CO_3).

At reaction temperatures of 600°C and 700°C , new sharp bands associated with other sodium silicate species such as sodium disilicate ($\text{Na}_2\text{Si}_2\text{O}_5$) and sodium pyrosilicate ($\text{Na}_6\text{Si}_2\text{O}_7$) appear. These results are consistent with those obtained by NMR, XPS and FT-IR analysis, indicating formation of more complex sodium silicate species such as $\text{Na}_2\text{Si}_2\text{O}_5$ ($\text{Na}_2\text{O} \cdot 2\text{SiO}_2$) and $\text{Na}_6\text{Si}_2\text{O}_7$ ($3\text{Na}_2\text{O} \cdot 2\text{SiO}_2$) at higher reaction temperatures. These observations are also confirmed by other scientific works.

V.3.3. Test of solid activators for the manufacture of one-part geopolymers based on light ash and addition of red mud

V.3.3.1. Compressive strength

Figure 33 shows the compressive strength of one-part geopolymers prepared with the solid activators synthesized in this paper.

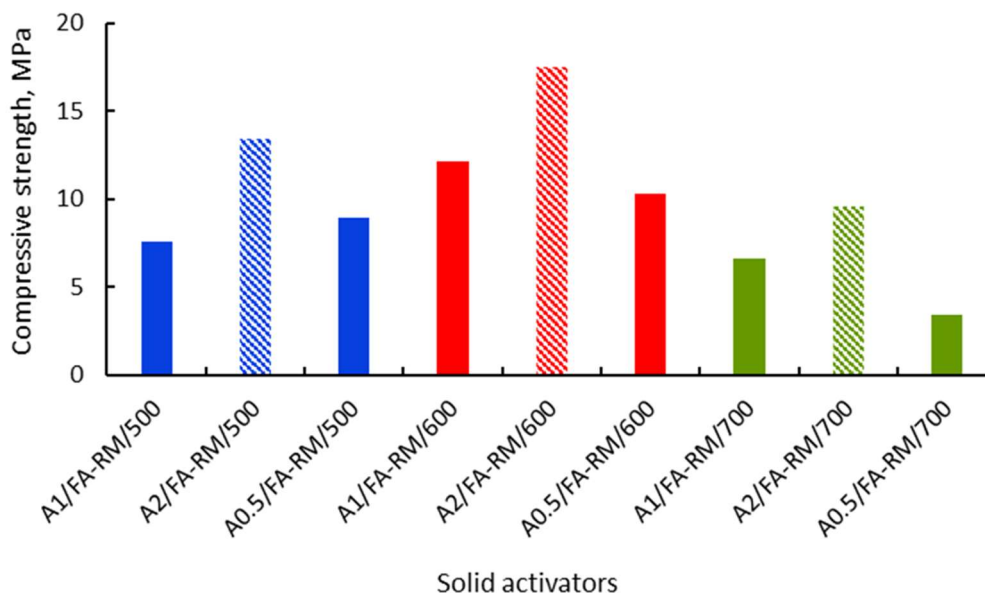
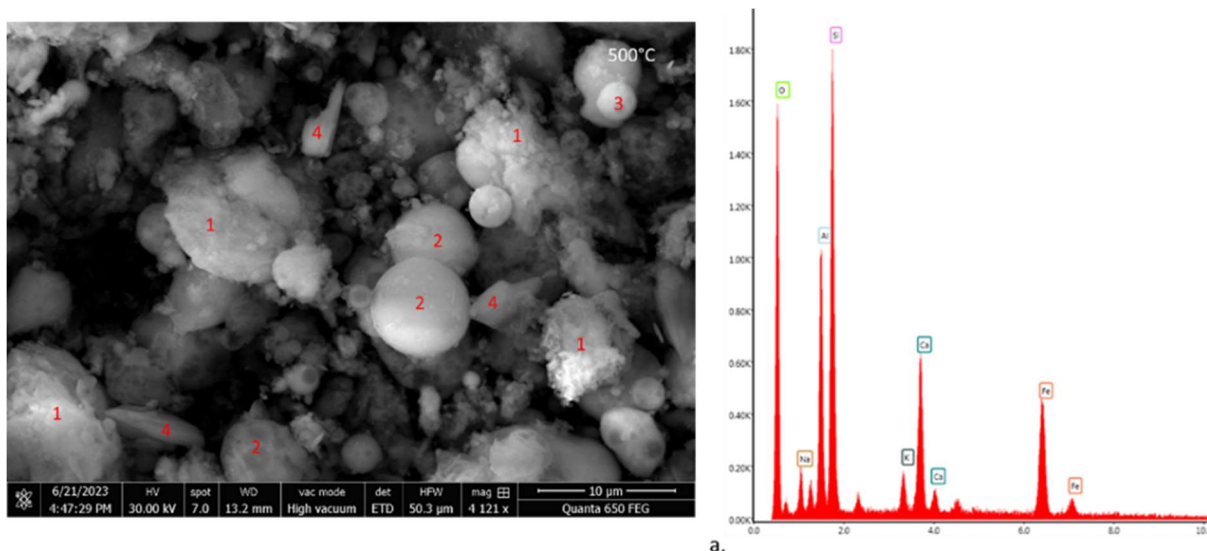


Figure 33. Compressive strength of one-part geopolymers.

The results on the compressive strength of solid activators are consistent with their solubility in water. Materials prepared with solid activators synthesized at a NaOH:CRT mass ratio of 2 and reaction temperatures of 600 °C have the best compressive strength. The water solubility of solid activators is a defining property that influences the properties of one-part geopolymers. The synthesis temperature of 600°C gives the best results, regardless of the initial mass ratio of the reactants. The compressive strength of A2/FA-RM/600 is 1.3 times higher than that of A2/FA-RM/500 and 1.8 times higher than that of A2/FA-RM/700. Next, the three types of "one-part" geopolymers with the best solubility in water will be characterized.

V.3.3.2. SEM-EDX analysis

SEM micrographs and EDX spectra of one-part geopolymers are shown in Figure 34.



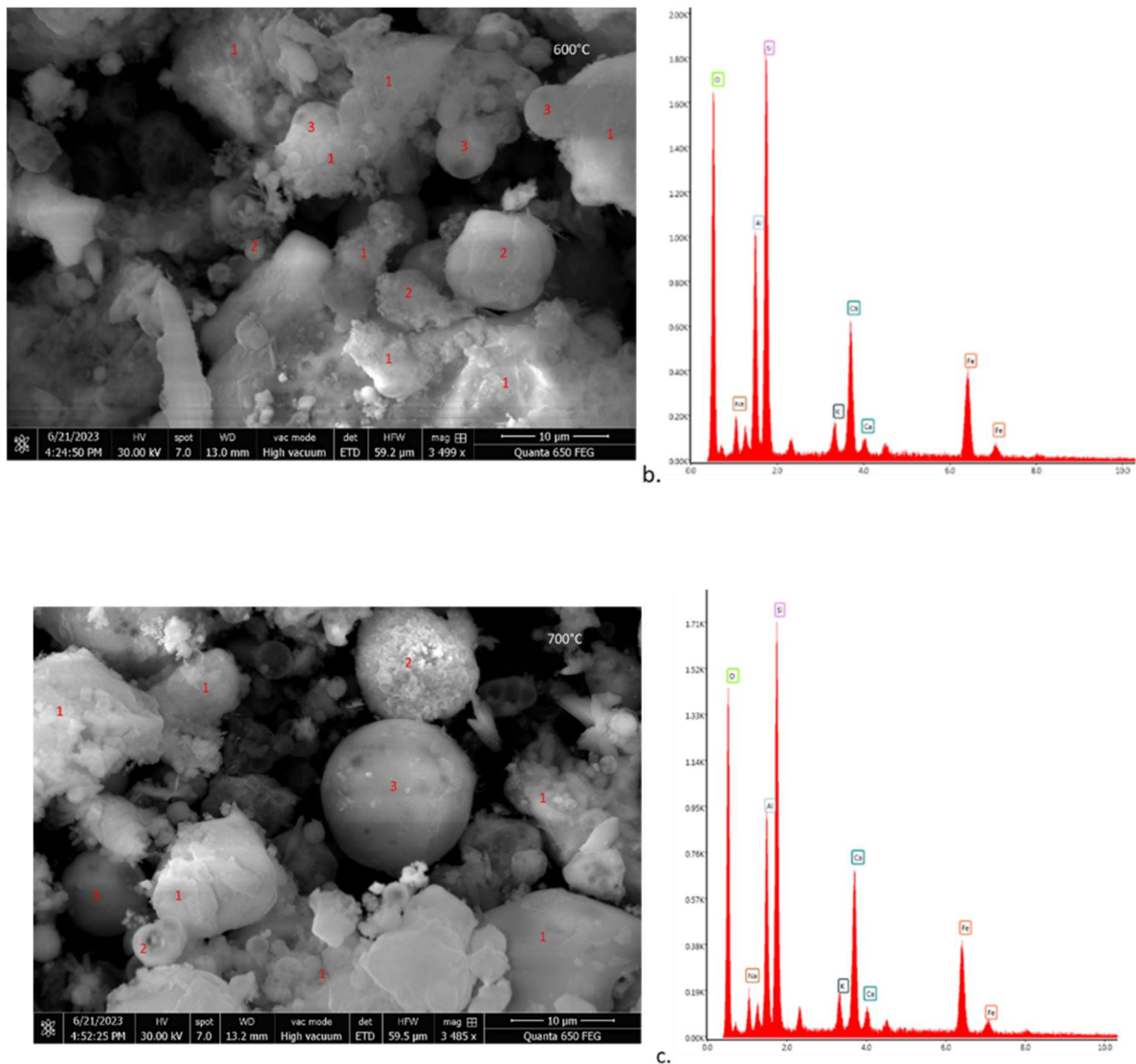


Figure 34. Micrographs and EDX spectra of „one-part” geopolymers: a. A2/FA-RM/500; b. A2/FA-RM/600; c. A2/FA-RM/700.

Micrographs of assortments A2/FA-RM/500, A2/FA-RM/600 and A2/FA-RM/700 reveal differences in the structure of aluminosilicate amorphous material. The A2/FA-RM/500 assortment features areas with amorphous material and spherical particles partially coated with amorphous gel. The A2/FA-RM/600 assortment has a more extensive mass of amorphous material and a lower proportion of light ash particles coated with amorphous gel. The A2/FA-RM/700 assortment features a less compact amorphous mass and completely unreacted light ash particles.

EDX analysis indicates changes in the composition of the phases of the amorphous gel depending on the type of solid activator used. The A2/FA-RM/600 assortment has a composition suggesting a better developed aluminosilicate network with a molar Na/Al ratio close to the unit. This comes closest to the theoretical optimal molar ratio Na/Si required for load balance in the connecting network. All three assortments indicate the possible formation of a gel with low calcium content. These observations are consistent with the literature.

V.3.3.3. FT-IR analysis

FT-IR spectra of solid activator assortments show that the main absorption band falls in the range of 973-980 cm^{-1} , attributed to the asymmetric stretching vibration of Si-O-Si or Si-O-Al bonds in aluminosilicate phases. There is a shift of this band towards a

higher wave number from 973 cm^{-1} for the A2/FA-RM/500 grade to 980 cm^{-1} for the A2/FA-RM/600 grade, indicating a higher degree of polymerization of the aluminosilicate phases. This is inversely proportional to the compressive strength. The absorption bands in the range $1422\text{--}1431\text{ cm}^{-1}$ are attributed to the O-C-O stretching vibration of carbonate groups. The absorption bands at approximately 1645 cm^{-1} and 3365 cm^{-1} are attributed to the bending vibration of the H-O-H bonds and the tension vibration of the O-H, respectively.

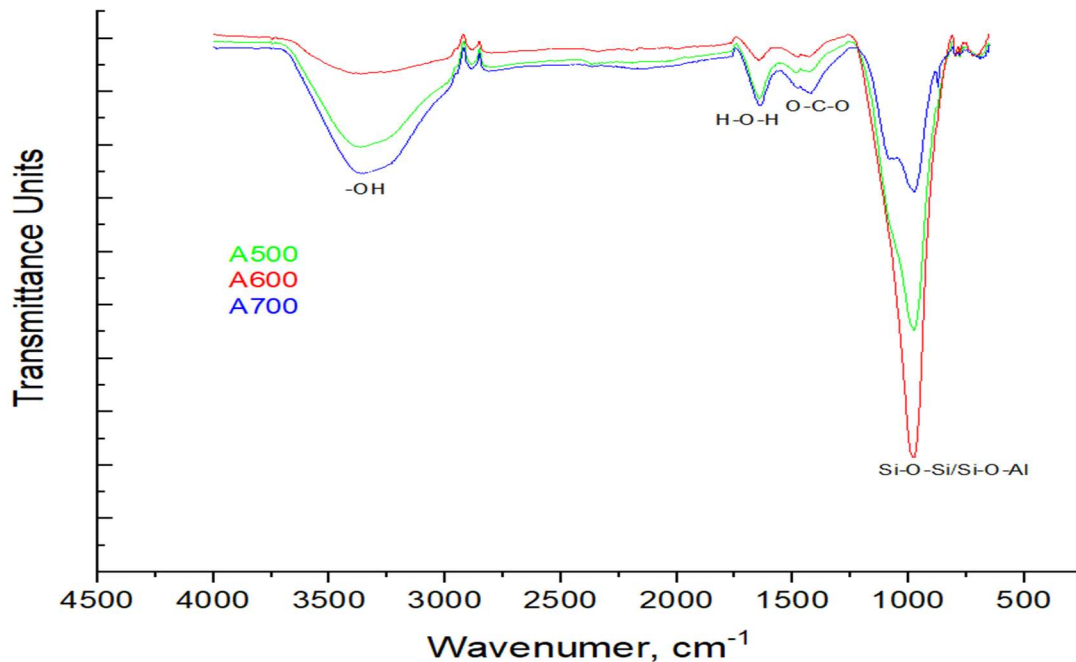


Figure 35. FT-IR spectra of „one-part” geopolymers.

V.4. Partial conclusions

The purpose of this chapter was to synthesize, characterize, and test a new class of alternative solid alkaline activators based on CRT glass waste. The synthesis of the solid activators was carried out by alkaline fusion with sodium hydroxide, and their testing was performed by preparing “one-part” type geopolymeric cements based on light ash and red mud. The results regarding the synthesis of the solid activators showed that the reaction temperature plays an important role in terms of their composition and characteristics. As the morphological and spectroscopic analyzes have proven, the assortments of solid activators synthesized at a temperature of 600°C have a composition similar to that of metasilicates, which gives them better solubility in water compared to other assortments of solid activators synthesized at other reaction temperatures. It seems that, at the synthesis temperature of 500°C , the CRT glass is below the vitreous transition temperature, the reaction probably being incomplete due to the lack of homogeneity of the reaction mixture, while at the synthesis temperature of 700°C more complex silicate species are formed, which give the solid activators a high degree of polymerization and, therefore, poor solubility in water.

The morphological and spectroscopic analyzes, as well as the compression resistance tests, showed that the “one-part” type geopolymers prepared with solid activators synthesized at the reaction temperature of 600°C have superior characteristics to the other assortments of solid activators. The assortment synthesized at this reaction temperature and at a mass ratio NaOH:CRT of 2:1 presents the most compact amorphous aluminosilicate structure, which gives it the best compression resistance.

Chapter VI. Evaluation of long-term leaching behavior of one-part geopolymers based on conformity leaching tests

VI.1. Specific objectives

The main objectives of this chapter were:

- ✓ Testing the leaching behavior of the most advanced geopolymers previously obtained, in relation to the heavy metals contained in the raw materials used for their preparation, by means of the TCLP (Toxicity Characteristic Leaching Procedure) compliance test;
- ✓ Calculation of real diffusion coefficients of heavy metal ions using the results of leaching tests and a diffusional model adapted to the leaching test used;
- ✓ Correlating the results obtained regarding the real diffusion coefficients calculated from experimental data with the results obtained using a theoretical model of their calculation;
- ✓ Establishing the degree of mobility of metal ions in tested geopolymers based on the obtained results and evaluating their long-term leaching potential.

VI.2. Materials and methods

VI.2.1. Material

To synthesize solid activators through alkaline fusion reaction, glass waste (shards) from cathode tubes (CRT), supplied by a company that collects and processes waste from electrical and electronic equipment (WEEE), as well as sodium hydroxide (98%, granular, analytical grade) were used. The oxide composition of the raw materials is presented in Table 16.

Before being used, the glass material was ground to a powdery state in a ball mill. Light ash, supplied by a local thermal power plant, and red mud, supplied by a local alumina refining industry, were used as precursor materials to prepare “one-part” type geopolymers. Before being used, the red mud was dried and ground to a powdery state.

VI.2.2. Synthesis of solid activators

The prepared prepared coded solid alkaline activators are shown in Table 17.

Table 17. The composition of the assortment of solid activators.

Code	Synthesis temperature, °C	NaOH/glass ratio (S/G), (m)
S/G 0.5	600	1:2
S/G 1		1:1
S/G 2		2:1

For the preparation of solid alkaline activators, glass waste powder and NaOH granules were mixed at three different mass ratios until a homogeneous mixture was obtained, then kept for 2 hours in an electric furnace at 600°C for alkaline fusion. The synthesized solid alkaline activators were cooled and finely ground.

VI.2.3. Preparation of test “one-part” geopolymers

The “one-part” geopolymers were prepared by dry mixing of light ash with red mud and solid activator until a homogeneous mixture was obtained. The solid activator/light ash-red mud mass ratio was set at 0.2. Subsequently, water was added to the formed

mixtures at a water/solid mass ratio of 0.5, and mechanically mixed until a homogeneous paste was obtained. The “one-part” geopolymers obtained are coded and presented in Table 18.

Table 18. The composition of "one-part" geopolymers.

Assortments	Fly ash, % (by mass)	Red mud, % (by mass)	Solid activator, % (mass)
S/G0.5/FA-RM/600	85	5	10
	80	10	
	75	15	
S/G1/FA-RM/600	85	5	
	80	10	
	75	15	
S/G2/FA-RM/600	85	5	
	80	10	
	75	15	

The pasta was poured into cylindrical polypropylene formwork measuring 5 cm (d) x 10 cm (l) and vibrated for 2 min. The formwork was then sealed in plastic bags and dried at 80°C for 28 days (after the first 24 hours of drying, the samples were deciphered, sealed in other plastic bags and then allowed to harden for the next 27 days).

VI.2.4. Leaching tests

Leaching behavior testing was performed by means of the TCLP leaching compliance test (USEPA, 1992). In summary, this test involves grinding samples to a particle size of less than 9.5 mm and mixing them with the leaching solution (acetic acid solution at pH 3) at a solid/liquid ratio of 1/21 for 18 hours. Next, the samples were filtered and prepared to measure the concentration of heavy metal ions (all heavy metals appearing in the composition of the secondary raw materials used) by atomic absorption in flame using a GBC 932 AA atomic absorption spectrometer with standard calibration solution for each heavy metal ion.

VI. 3. Results and discussion

VI.3.1. Description of the leaching model

There are several simple leaching models that are constructed by adopting a series of initial assumptions, such as:

- Contaminants do not participate in reactions,
- The leaching bath is infinite,
- The solid from which contaminants leachate is infinite,
- Contaminants are homogeneously distributed in the solid phase prior to leaching.

Experimental data for such models come from dynamic leaching tests, in which the tested solid is in the form of a monolith. Based on these assumptions, the material balance equation can be solved, thus establishing the concentration profile of contaminants inside the solid, as shown in equation (1), where M_t/M_0 is the fraction of leachate contaminant at time t , D_e is the effective diffusivity of the contaminant, L is the

distance from the outside of the monolith to its centre and t is the moment at which leaching began [13].

$$\frac{M_t}{M_0} = \left(\frac{4D_e}{\pi L^2} \right)^{0.5} t^{0.5} \quad (1)$$

However, in many cases, contaminants participate in reactions inside the solid during leaching. This is also the case with heavy metal ions which, depending on the characteristics of the solid, can participate in specific reactions. Therefore, equation (1) could be rewritten (2) in terms of observable diffusivity (D_{obs}) instead of effective diffusivity (D_e). When the fraction of mobile contaminant (F_m) is small in the solid at the beginning of the leaching process, it follows that for precipitation/dissolution reactions D_{obs} is expressed by equation (3), while for sorption reactions it is expressed by equation (4).

$$\frac{M_t}{M_0} = \left(\frac{4D_{obs}}{\pi L^2} \right)^{0.5} t^{0.5} \quad (2)$$

$$D_{obs} = \frac{\pi F_m D_e}{2} \quad (3)$$

$$D_{obs} = F_m D_e \quad (4)$$

These models can also be adapted for TCLP leaching test conditions. Thus, if L in equation (2) is approximated to the volume/area ratio of particles (V_p/A_p), then equation (2) can be written in terms of contaminant concentration both after leaching and before leaching as shown in equation (5), where C_0 is the initial concentration of the contaminant in solid (g/kg) and M_p/V_l is the solid/liquid ratio corresponding to the TCLP leaching test.

$$C_{TCLP} = C_0 \frac{M_p}{V_l} \frac{A_p}{V_p} \left(\frac{4D_{obs}}{\pi} \right)^{0.5} t^{0.5} \quad (5)$$

The main problem is that in the TCLP leaching test, acetic acid is used as a leaching solution at a pH of 3 or 5 depending on the characteristics of the material being leached. This could lead to an increase in the leaching rate of contaminants because acetic acid migrating inside the solid reacts with contaminants. Under these conditions, the observable diffusivity will depend on the concentration of acetic acid used for leaching as shown in equation (6), where C_0 is the concentration of immobile contaminant at the beginning of leaching $D_{e,Ac}$ is the effective diffusivity of acetic acid, C_{Ac} is the concentration of acetic acid and n is the ratio of acetic acid reacting to dissolve the contaminant.

$$D_{obs} = \frac{\pi D_{e,Ac} C_{Ac}}{2n C_0} \quad (6)$$

Under these conditions, the leaching of contaminants is described both in terms of the characteristics of the leaching solid and the characteristics of the leaching solution. However, estimating the effective diffusivity of species participating in the leaching process (acetic acid and contaminants) in solid is an important issue. Since this cannot be calculated from the results of leaching tests (it would be necessary to adopt the hypothesis that contaminants do not react inside the solid during the leaching process, which is not the case here), the best method of determination remains the one based on measurements of the electrical conductivity of both the solid and the aqueous solution in its pores (Taffinder and Batchelor, 1993). The ratio of the conductivity of the solid to the conductivity of the aqueous solution in the pores represents MacMullin's number, and this, in turn, is equal to the ratio of molecular diffusivity to effective diffusivity of species of interest in the leaching process, as shown in equation (7).

$$N_M = \frac{D_m}{D_e} \quad (7)$$

It is worth mentioning that in this work the calculation of contaminant mobility in the obtained geopolymers was made based on the results of leaching compliance tests (TCLP test) and the leaching model adapted to the conditions of this leaching test, which is a novelty in the field for such materials.

V.3.2. TCLP test results

The results of TCLP tests performed on “one-part” geopolymers are shown in Figure 36. As can be seen, these materials have a very low leaching capacity compared to contaminants present in the raw materials used in their preparation (Table 16).

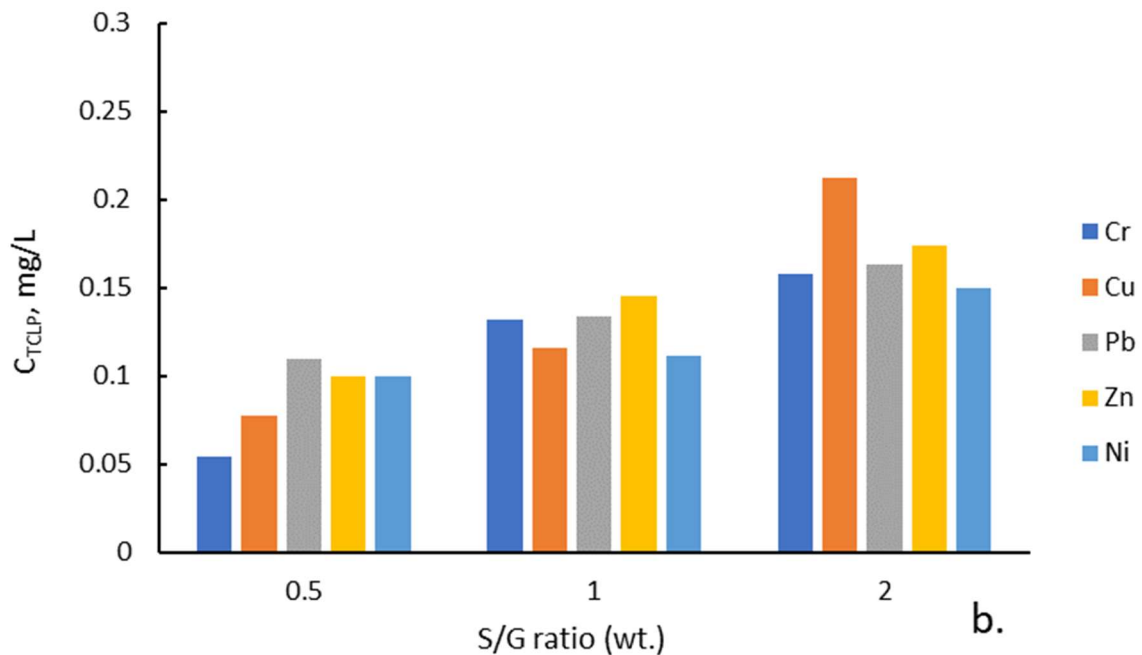
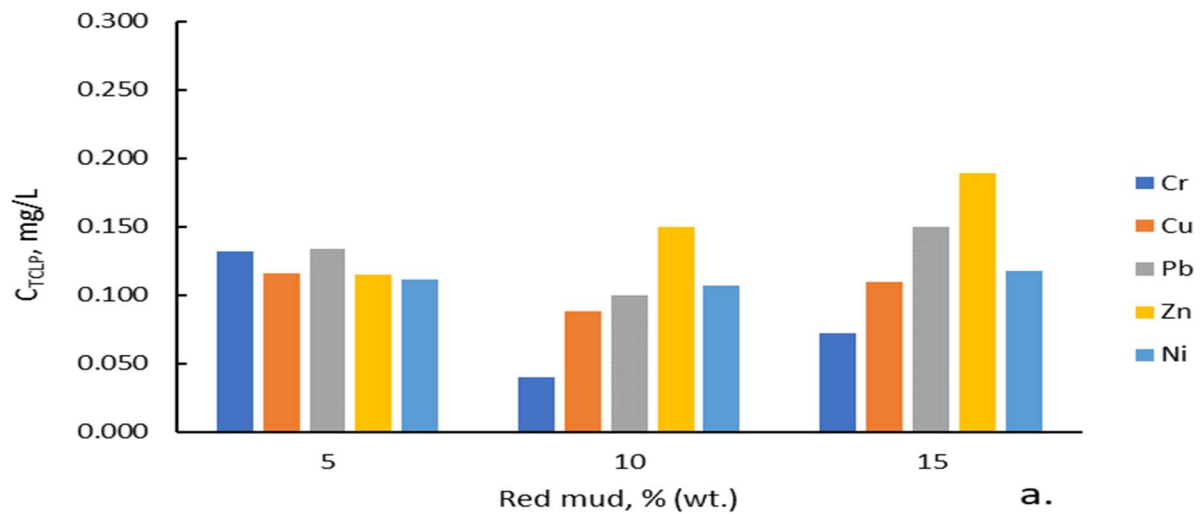


Figure 36. TCLP test results: a. Leachate concentration of contaminants as a function of proportion of red mud added to the synthesis mixture; b. Leachate concentration of contaminants as a function of the mass ratio of sodium hydroxide/glass CRT (S/G) to be used in the synthesis of solid activators.

The highest concentration of Cr measured in leaching solutions (0,158 mg/L) is approximately 30 times lower than the limit concentration set by the standard (5 mg/L). The same result was recorded for Pb (0,163 mg/L in leaching solution versus 5 mg/L, limit concentration set by the standard). These results clearly indicate that the materials obtained are not hazardous in relation to the heavy metals contained.

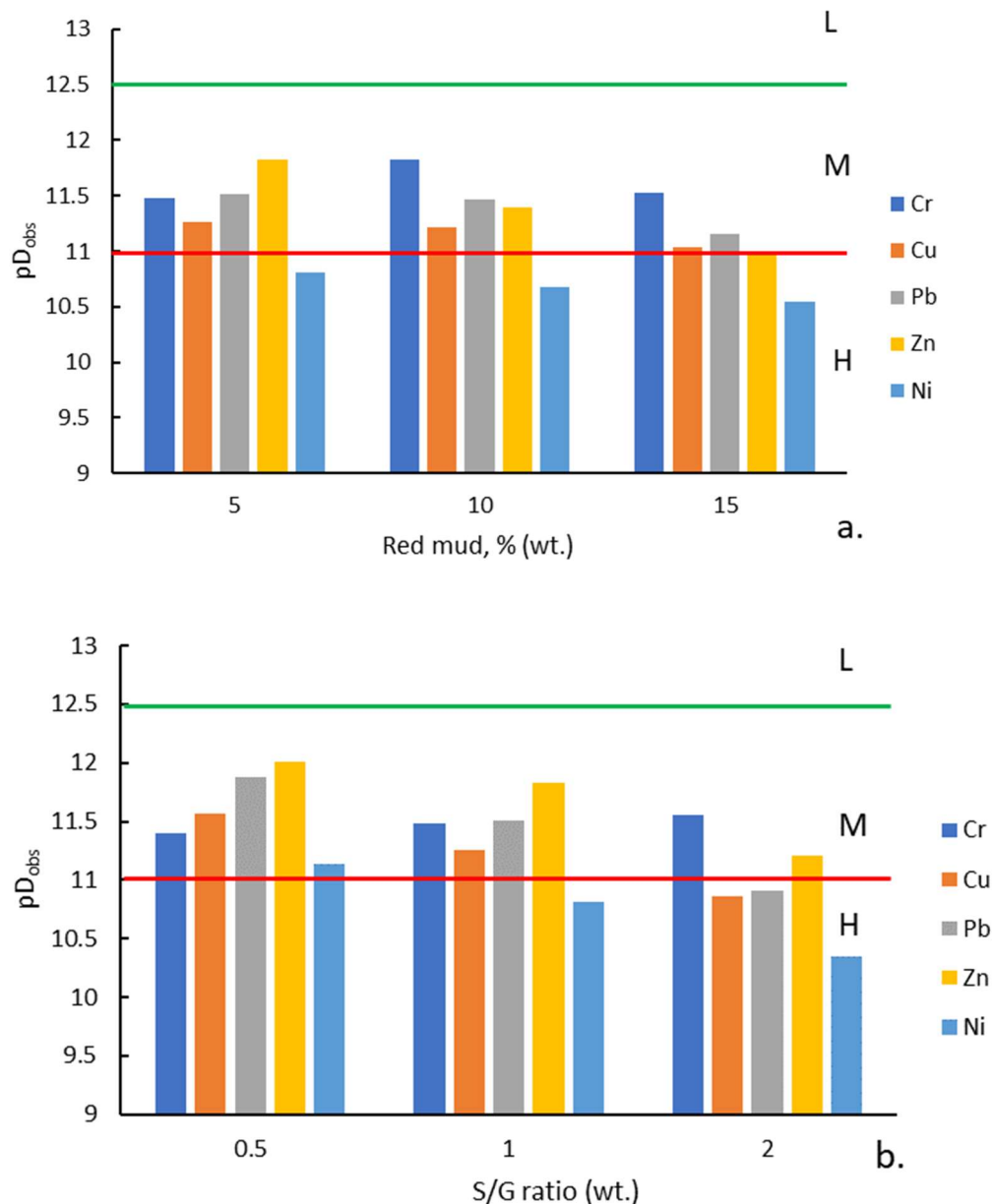


Figure 37. Assessment of contaminant mobility a. Mobility according to the proportion of red mud added to the synthesis mixture; b. Mobility according to the proportion of sodium hydroxide/CRT glass (S/G) used in the synthesis of solid activators; H-high mobility, M-medium mobility, L-low mobility.

Figure 37 shows the mobility of contaminants in one-part geopolymers, expressed as the negative logarithm of observable diffusivity ($-\log D_{\text{obs}}$ or pD_{obs}), depending on the conditions of synthesis of solid activators and preparation of geopolymers. The results indicate that only nickel has high mobility, except for the S/G 0.5 grade. At the medium/high mobility limit is the case for copper and zinc for grades with 15% red mud and copper and lead for grades S/G 2 (Figure 37 a and b). Note that the higher the logarithm value of observable diffusivity, the lower the mobility of the contaminant in the solid material.

VI.3.3. Assessment of long-term leaching behaviour

It is expected that adding an increasing amount of strongly alkaline red mud will increase the total alkalinity of the prepared geopolymers. Consequently, the solubility of contaminants should increase as a result of the increase in the pH of the interstitial solution of the solid ($\text{pH} > 11$), forming oxyanions such as $\text{Pb}(\text{OH})^{-3}$, $\text{Pb}(\text{OH})_4^{-2}$, $\text{Cu}(\text{OH})^{-3}$, $\text{Zn}(\text{OH})^{-3}$ etc. (Bobiričă et al., 2018). A similar case is when the S/G ratio increases in the synthesis of solid activators. Upon contact of the solid with the acidic leaching solution, the pH of the pore water begins to decrease, and the contaminants will precipitate again, probably in the form of their hydroxides. As the acid diffuses into the solid, the contaminants will dissolve again, forming a precipitation/redissolution front inside the solid particle that migrates from the outside to the inside of it (Park and Batchelor, 2002). This could be the explanation for the increase in the mobility of contaminants, with the exception of chromium, with the increase in the proportion of red mud added, respectively with the increase in the mass ratio sodium hydroxide/glass in the synthesis of solid activators (Figure 36). Regarding the evaluation of the leaching behavior of chromium, it is possible to find it mainly in hexavalent form (CrO_2^{-4}) and thus to be less influenced by the variation of the pH of the aqueous solution in the pores. However, it could participate in sorption processes competing for active areas on the surface of the solid phases of the geopolymeric matrix with the acetate ions from the leaching solution (Park et al., 2006). As can be seen in Figure 37, the mobility of chromium does not have a clear trend of increase or decrease depending on the alkalinity of the system. To verify these explanations, the results regarding the mobility of contaminants obtained from the leaching tests were compared with those obtained with the reactive leaching model which takes into account the participation of acetic acid from the leaching solution in the reactions (precipitation/dissolution or sorption) with the contaminants in the solid during the leaching process. Thus, this comparison is presented in Figure 38, specifying that the MacMullen number necessary to calculate the effective diffusivity of acetic acid for particles smaller than 10 mm was obtained by interpolation from data in the specialized literature (Figure 39).

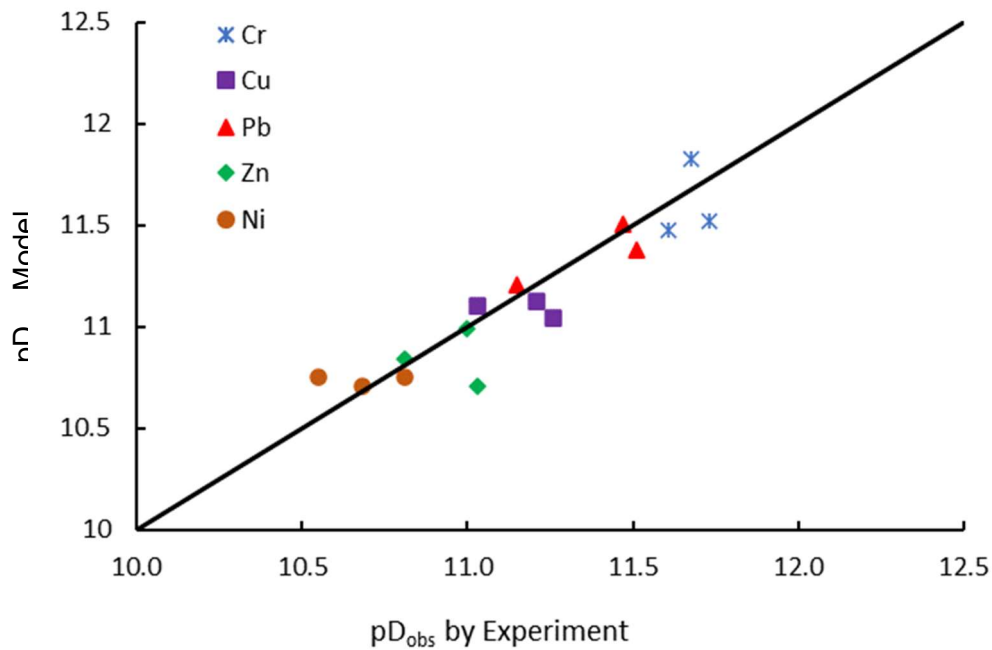


Figure 38. Comparison of mobility predicted by the reactive model with that calculated from TCLP test results.

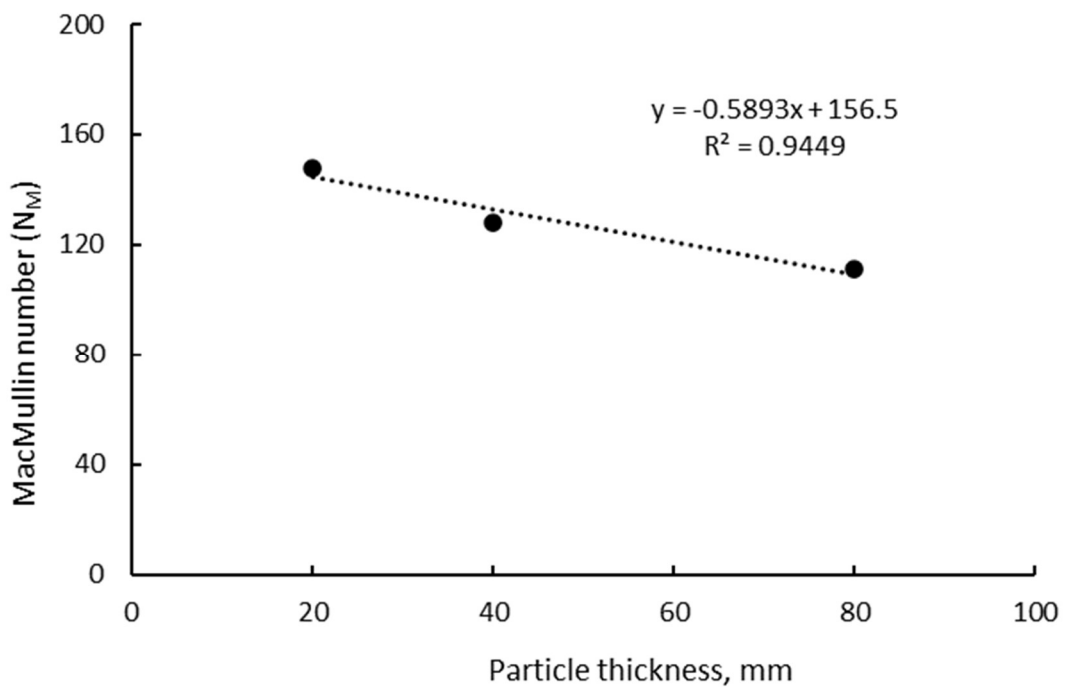


Figure 39. Estimation of MacMullin number by interpolation from literature data.

As can be seen from Figure 39, there is a good correlation between the two datasets for all contaminants considered in this paper. However, there is a tendency for mobility in some metals to be underestimated, which could indicate that some metal species under certain conditions precipitate in a somewhat more stable form than their hydroxides or may be taken up by solid phases of the system.

VI.4. Partial conclusions

This chapter evaluated the leaching behavior of contaminants from “one-part” type geopolymers, using data from conformity leaching tests (TCLP). The results indicate a medium, sometimes high, mobility of contaminants, depending on the characteristics of the material. Although the conformity tests show a reduced capacity of leaching contaminants, the increase in the alkalinity of the system by adding alkaline raw materials generally increases the mobility of contaminants. The participation of acetic acid from the leaching solution in reactions with contaminants was confirmed by comparing the experimental data with those of the reactive leaching model, obtaining a good correlation. The conclusion is that more attention should be paid to the development of conformity leaching tests for different materials and waste in the future, in order to correctly evaluate the long-term leaching behavior.

VII. General conclusions

The experimental results demonstrate that industrial waste and by-products can be used as secondary raw materials for the manufacture of ecological geopolymers, an alternative to Portland cement-based materials. The direct and indirect use of glass has highlighted its potential in geopolymerization processes and the synthesis of solid alkaline activators. The performance of geopolymers and activators varies depending on the amount of glass added and the parameters of the synthesis process. Geopolymers prepared with an optimal addition of glass waste and with activators with a predominantly metasilicate composition have demonstrated a high capacity to immobilize mercury and a reduced potential for long-term leaching of contaminants, confirming their non-hazardous nature. These results underline the high potential for valorizing hazardous glass waste in the production of geopolymers and other ecologically alkaline activated materials for use in the industrial sector.

Original contributions and prospects for further development

The novelty elements presented in the experimental research related to the doctoral thesis are:

1. Synthesis of ecological “two-part” type geopolymers based on light power plant ash with the addition of glass waste from out-of-use fluorescent lamps without a preliminary treatment of them, in the sense of removing the fluorescent powder generically called “phosphorus” with a high mercury content;
2. Designing an original system for processing fluorescent lamps taken into work to safely capture the mercury vapors present in them during their breaking in order to obtain crushed glass waste which will later be ground to obtain glass powder;
3. Development of an original procedure by designing synthesis mixtures, based on which the initial molar ratios between the main oxides of the system can be calculated with the highest accuracy and subsequently, their optimization can be achieved;
4. Highlighting the potential of the obtained geopolymers to immobilize mercury from glass waste through conformity leaching tests;
5. Synthesis of new assortments of solid alkaline activators based on glass waste from out-of-use cathode tubes (CRT) by alkaline fusion with the optimization of synthesis parameters;
6. Synthesis of ecological “one-part” type geopolymers based on light power plant ash and red mud using new assortments of solid alkaline activators based on CRT type glass waste;
7. Estimation of the mobility of contaminants in the obtained geopolymers, based on conformity tests and suitable leaching models.

The results obtained in the doctoral thesis open the following research perspectives in this field:

1. Expansion of the range of industrial waste and by-products to be used as precursors for the synthesis of ecological geopolymers;
2. Expansion of the range of industrial waste and by-products on the basis of which to synthesize solid activators with potential for use in the synthesis of one-part type geopolymers;
3. Correlation of the results of conformity leaching tests with those of dynamic leaching tests, in order to develop a mathematical model based on which the long-term mobility, under various environmental conditions of the contaminants in the synthesized geopolymers, can be estimated with the highest accuracy;
4. Identification of the mechanisms of immobilization of contaminants in geopolymeric systems, so that synthesis mixtures can be designed that lead to final products as safe as possible from the point of view of environmental protection.